SIGNAL AND NOISE CHARACTERISTICS OF PHOTOVOLTAIC P-N JUNCTION DIODES

by

DONALD STEWART GALBRAITH

B. A., University of British Columbia, 1955

A THESIS SUBMITTED IN PARTIAL FULFILMENT OF THE REQUIREMENTS FOR THE DEGREE OF MASTER OF SCIENCE

in the Department

of

Physics

We accept this thesis as conforming to the required standard

THE UNIVERSITY OF BRITISH COLUMBIA

December, 1957

ABSTRACT

The noise characteristics of ideal photovoltaic p-n junction diodes are discussed and investigated. The hypothesis is advanced that the open-circuit noise from an illuminated ideal diode is entirely due to the shot noise of the various current contributions. Theoretical justification for this theory is developed and the parameter t, the effective noise temperature ratio, is introduced. The possible reasons for excess noise in p-n photo-diodes observed in earlier experiments are suggested.

The dc and ac behavior of a real diode chosen to be very nearly ideal in its dc characteristic is found to be consistent with existing diode theory. The various parameters appropriate to the device are evaluated.

Equipment for noise measurement is selected and a comparison technique adopted. This method avoids many of the possible errors inherent in an absolute measurement and allows an equivalent noise resistance resolution of about 200 ohms at room temperature in the 200 cs bandwidth measured. The open-circuit noise of the selected diode is measured at 20 and 30 kc as a function of illumination and the results interpreted in terms of the equivalent resistance in thermal equilibrium which would give the same noise. Comparison of this set of values with the real part of the junction impedance in each case indicates that the theory advanced is adequate to predict noise under these circumstances.

The signal-to-noise ratio for a photo-diode used as an open-circuit radiation detector is developed, and several recommendations

are made regarding the design of a photo-diode to display the most favourable signal-to-noise ratio under illumination.

In presenting this thesis in partial fulfilment of the requirements for an advanced degree at the University of British Columbia, I agree that the Library shall make it freely available for reference and study. I further agree that permission for extensive copying of this thesis for scholarly purposes may be granted by the Head of my Department or by his representative. It is understood that copying or publication of this thesis for financial gain shall not be allowed without my written permission.

Department of Physics

The University of British Columbia,
Vancouver 8, Canada.

Date December 20, 1957.

TABLE OF CONTENTS

ACKNOWLEDGMENTS

I wish to thank Professor R. E. Burgess for his guidance throughout the course of this investigation and for his many valuable comments during the preparation of this thesis.

The work described was carried out under Defence Research Board grant number 9512-22. I also wish to thank the Board for personal financial assistance from April to December of 1957.

I am indebted to Mr. D. A. McCoy for his assistance in the preparation of the figures.

D. S. G.

Facing Page 1

FIGURE 1

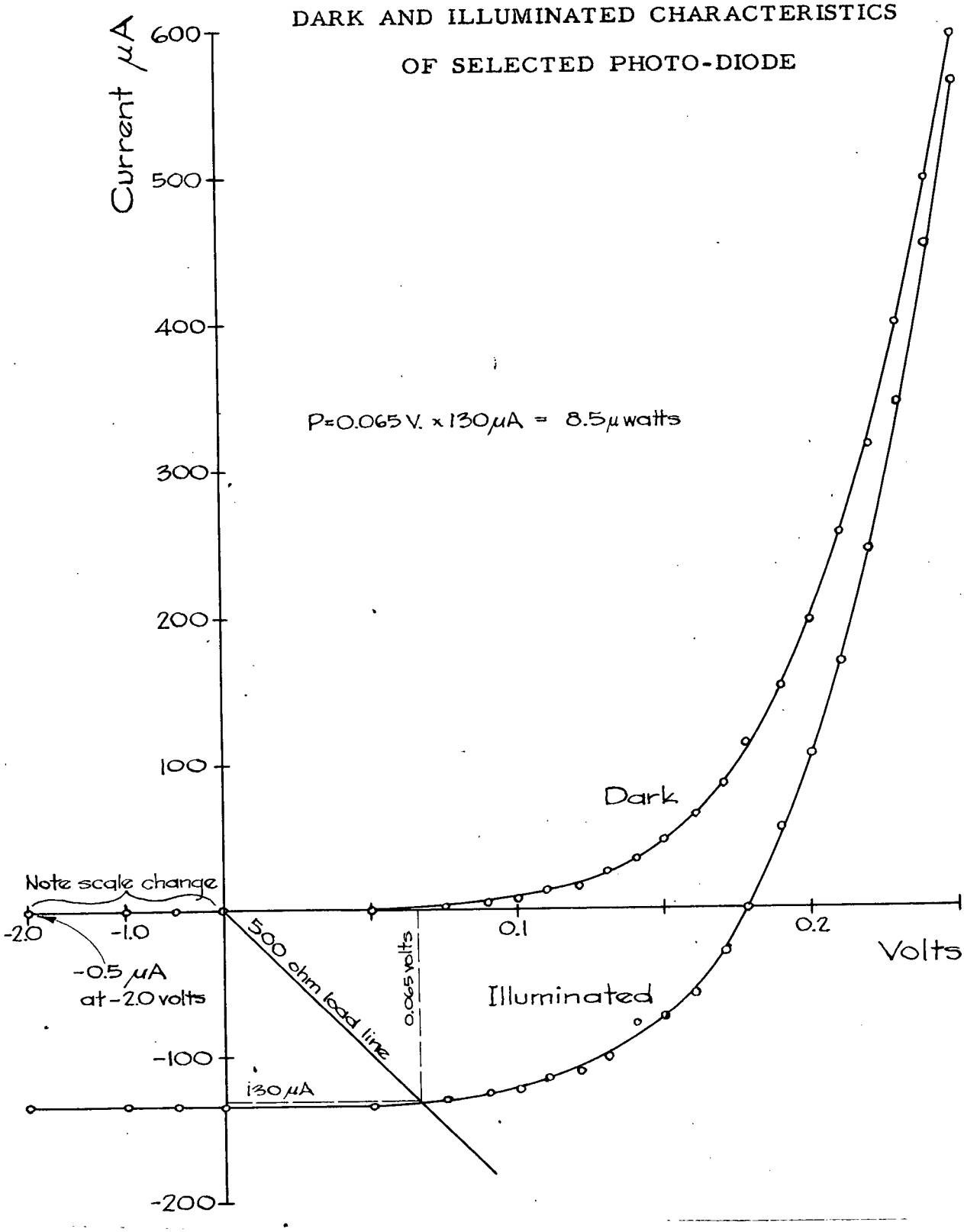

CHAPTER 1 - INTRODUCTION

1.1 Review of Previous Work

Briefly, a photovoltaic p-n junction diode is a solid state device capable of converting incident illumination (of suitable wavelength) into electrical energy. Its operation as a circuit element can best be outlined by reference to figure 1. The dark characteristic plotted here is similar to that of an ideal diode. Shockley (1949) has derived the following relation between current (I) and voltage (V) for an ideal p-n junction diode;

$$I = I_o(\exp\frac{qV}{kT} - 1), \tag{1}$$

where I_o = reverse saturation current
q = electronic charge
k = Boltzmann's constant
T = absolute temperature of junction.

To do so he assumed that the transition region between n and p regions has negligible width compared to the diffusion lengths of the carriers, and that the currents involved are small (such that the injected carrier density in either region is small compared to the density of the carrier normally present therein).

Later Cummerow (1954) considered the case occurring when photons of energy greater than the energy gap of the semiconductor fall on or near the junction creating hole-electron pairs which, crossing the junction unsymmetrically because of the electrostatic field existing there, constitute an additional current. He showed that the current flow in this case is given by

$$I = I_o(\exp\frac{qV}{kT} - 1) - BL \tag{2}$$

where BL, the photocurrent, is proportional to the incident light

intensity L. In other words, the illumination causes a proportional current contribution in the opposite direction to the forward dark current. In effect, then, illumination drops the diode's dark characteristic by an amount BL, as is indicated by the curve in figure 1 for an illuminated device.

That portion of the curve falling in the fourth quadrant is of particular interest because it is the portion generated by the illuminated device and a passive load alone. The point of intersection of the appropriate illuminated characteristic with a load line drawn from the origin indicates the voltage across and current through that load under that illumination and thus shows the power delivered to the load. For example, the diode tested would deliver about 8.5 microwatts (130 μA at 65 mv) to a 500 ohm load at the illumination level plotted.

It should be noted that real devices (including that for which figure 1 was plotted) exhibit various departures from ideal behavior. Several of these departures will be considered in later sections.

Although these diodes are finding numerous applications as radiation detectors or energy convertors, relatively little attention has been paid to certain aspects of their properties. In particular, no thorough investigation of their noise behavior under illumination has been performed.

Several sets of measurements have been made, however. Gianola (1956) investigated silicon broad area junctions under open-circuit conditions at various incident light intensities and in the frequency range from 20 cs to 4 kc. His results indicate a 1/frequency noise voltage squared spectrum under constant illumination and a varying

noise magnitude with varying illumination. This variation of noise voltage is quite marked and passes through a maximum which appears reasonably independent of frequency over the range investigated. He explained his results on the basis of current-dependent fluctuations of current.

Specifically, he assumes that the mean square current fluctuation is directly proportional to the photocurrent (BL in equation 2) and thus to the illumination; i. e.,

$$\overline{i^2} = sqBL\Delta f$$

where s is independent of the magnitude of the photocurrent but is a function of frequency. The measured mean square voltage fluctuation, however, is the product of this current fluctuation with the square of the dynamic impedance of the junction. This latter term decreases with increasing illumination (under open-circuit conditions) so the maximum in the noise voltage versus illumination plot is quantitatively reasonable.

Gianola's assumption for the form of the current noise is rather suggestive of the shot noise equation

$$\overline{i^2} = 2qI\Delta f \ .$$

Any attempt to apply this equation directly to a p-n junction, however, is complicated by the necessity of sorting out the contributions of the various carriers to the current and, assuming their individual motions to be essentially uncorrelated, adding up their contributions to the noise. Gianola's diode exhibited current noise of the order of 10^4 greater than that which would result from shot noise in a vacuum diode carrying a current equal to the p-n diode's photocurrent.

The objection might be raised that the broad area junctions used in this investigation are notoriously poor diodes, especially in that their reverse dc characteristics indicate a rather low shunt resistance. This being the case, the preceding study was not actually made under open-circuit conditions, since relatively heavy currents could flow internally.

To incorporate the non-ideal behavior of the device studied, Gianola fitted its characteristics to those predicted by the Bethe model (Torrey and Whitmer, 1948). The equation for the dc characteristics of this model differs from that of Shockley's (equation 1) by replacing the latter's I_o with a term $I_o \exp(-\beta \frac{qV}{kT})$, where $0 \leq \beta \leq 1/2$. Although there is a theoretical basis for its application to point-contact diodes, the equation can be applied to junction diodes only on empirical grounds. The effect of the extra factor is to lower the characteristic from the ideal (Shockley) curve for both forward and reverse bias, viz:

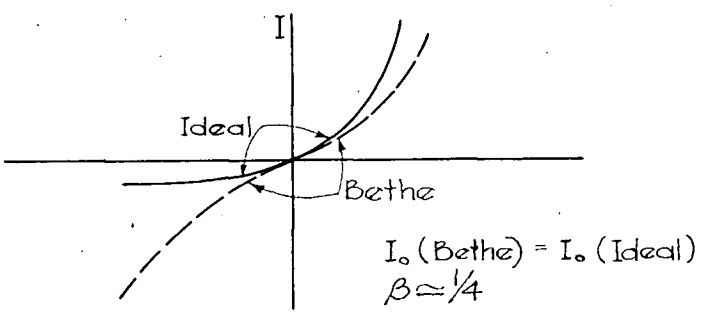

Poor reverse diode behavior, however, can generally be explained in terms of low shunt resistance, while reduced forward current indicates series resistance or high carrier injection (violating Shockley's assumption). Since the forward and reverse non-ideal characteristics stem from different causes, it is unreasonable to expect an additional term involving only one extra parameter to provide more than a rough,

empirical correction.

Another study by Pearson, Montgomery, and Feldmann (1955) points up one of the dangers encountered in this field. Their measurements indicate that a nearly ideal silicon p-n diode illuminated and reverse biased to give a current of the order of 10^4 times I_o exhibits precisely shot noise down to fairly low frequencies (80 cs). When the reverse saturation current is raised by a factor of about 100 by exposing the device to very humid air, the noise behavior changes markedly; exhibiting a 1/frequency current-squared spectrum with a 100 cs value about 10^5 above shot noise. These results indicate (as indeed the authors concluded) that excess noise in semiconductor devices can be a strongly surface-dependent property.

Noise measurements have been made on an InSb photovoltaic cell (Mitchell, Goldberg, and Kurnich, 1955) under illumination. A 1/frequency^3 noise voltage-squared spectrum is reported below 2 kc with substantially white noise (mean squared noise voltage constant with frequency) from 2 kc up to about 200 kc. Once again, however, the task of ascribing the noise generation to a simple mechanism is complicated by the non-ideal nature of the device which, according to the authors, 'exhibited . . . no noticeable rectification.'

1.2 Theoretical Considerations

At present, there is no all-embracing theory for the noise behavior of an ideal p-n photo-diode although several reasonable conjectures may be made. Obviously, Nyquist's theorem must apply to an open-circuited diode in the dark when in thermal equilibrium whether the noise is considered from the thermodynamic or the corpuscular point of view.

To illustrate this, consider an ideal Shockley diode in thermal equilibrium. Its characteristics are then given by equation 1 which may be interpreted as predicting a current $I_o \exp\frac{qV}{kT}$ in the forward direction and I_o in the reverse direction. If we assume these currents to be microscopically uncorrelated (or more exactly, if we assume the carrier transits comprising these currents occur independently and randomly at mean rates $\frac{I_o}{q}\exp\frac{qV}{kT}$ and $\frac{I_o}{q}$ respectively) we may write the shot noise equation as

$$\frac{\overline{i^2}}{\Delta f} = 2qI = 2qI_o(\exp\frac{qV}{kT} + 1).$$

Since we have postulated thermal equilibrium, V must be zero, so

$$\frac{\overline{i^2}}{\Delta f} = 4qI_o .$$

Differentiating equation 1 with respect to V and setting V equal to zero gives for the low frequency open-circuit conductance

$$G = \frac{\partial I}{\partial V} = \frac{qI_o}{kT}, \text{ or } qI_o = kTG.$$

With this substitution, the shot noise equation becomes

$$\frac{\overline{i^2}}{\Delta f} = 4kTG$$

which is Nyquist's thermodynamic result. Thus the thermodynamic and corpuscular approaches have been shown to be compatible in thermal equilibrium under the assumptions used.

FIGURE 2

ELECTROSTATIC POTENTIAL AND QUASI-FERMI LEVELS IN AN ILLUMINATED P^+-N JUNCTION

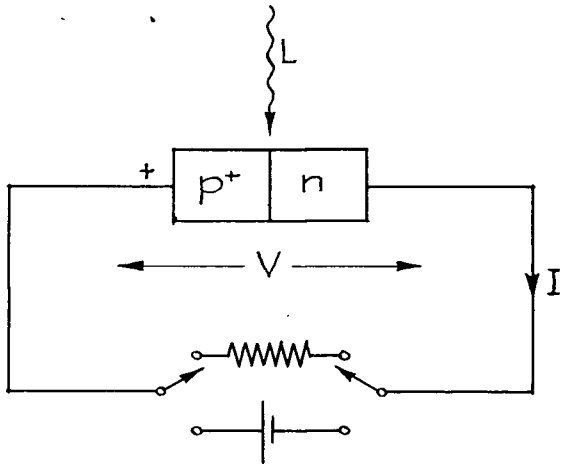

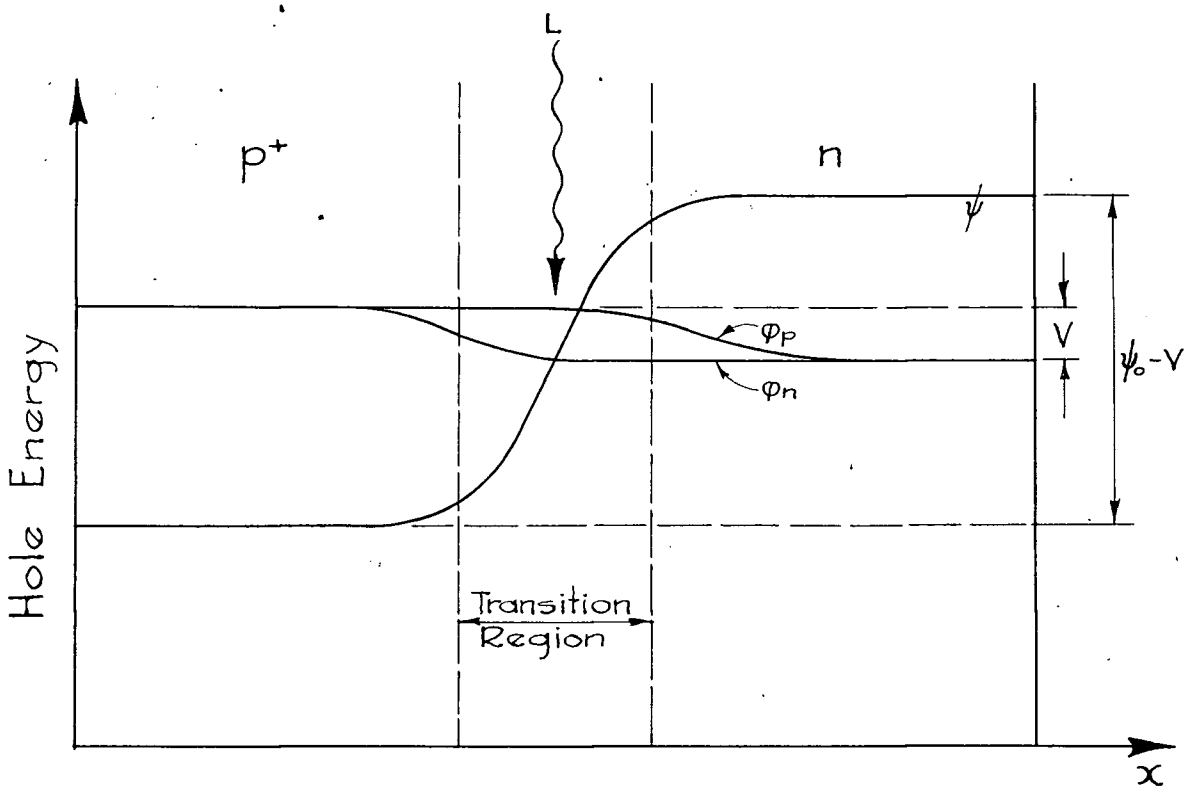

Under illumination, however, the situation could be more complicated. Let us first describe in general terms the usual photo-diode model. Figure 2 shows the internal distribution of the electrostatic potential ψ and the quasi-Fermi levels φ_p and φ_n (Shockley, 1949) for a one-dimensional model. Here V and I, the voltage across and current through the diode, are the same as those appearing in equation 2. For simplicity, the diode shown is p^+-n, rather than p-n, because under this condition virtually all the current in the n region at the junction is due to hole diffusion.

For small injected carrier densities, the reverse current arises from holes diffusing from the n to the p^+ region at a rate independent of the voltage across the junction but proportional to the number of holes available for such diffusion. Thus the reverse current is $I_o + BL$, where I_o, the macroscopic dark saturated reverse current, corresponds to the thermally generated holes and is proportional to the equilibrium density of holes in the n region p_n; being equal in fact (Shockley, 1949), to $Aqp_n\frac{D_p}{L_p}$, where A is the area of the junction and D_p and L_p are the diffusion constant and diffusion length respectively for holes in the n region. The BL term accounts for the extra light-created holes available for diffusion.

The forward current, on the other hand, arises from those holes in the p^+ region having enough energy to surmount the junction potential barrier. This barrier is lowered from its equilibrium height by the voltage V appearing across the diode, so the forward current will be a function of V and is, in fact, $I_o \exp\frac{qV}{kT}$.

It should be noted that the preceding discussion - subject

to the restrictive assumption of low injected carrier density - is quite independent of the cause of the voltage across the diode; this voltage may be applied by an external battery, may be the open-circuit photovoltage of the diode, or may be the photovoltage appearing across an arbitrary load.

If we assume, as in the equilibrium case, that the contributions to the total current are individually uncorrelated, we may write the shot noise equation for the illuminated case as

$$\frac{\overline{i^2}}{\Delta f} = 2q(I_o \exp\frac{qV}{kT} + I_o + BL).$$

We shall now introduce a new variable t, the effective noise temperature ratio, which we define as the ratio of the mean squared current or voltage noise in a particular case to that given by Nyquist's theorem applied to the conductance or resistance. Thus for current noise

$$t \equiv \frac{\overline{i^2}}{4kTG}.$$

Differentiating equation 2 with respect to V gives for the low frequency diode conductance under illumination

$$G = \frac{\partial I}{\partial V} = \frac{qI_o}{kT}\exp\frac{qV}{kT} = \frac{q}{kT}(I + I_o + BL), \tag{3}$$

and hence

$$t = \tfrac{1}{2}\left[1 + (1 + \frac{BL}{I_o})\exp(-\frac{qV}{kT})\right]. \tag{4}$$

To investigate the open-circuit case, I = 0 is substituted into equation 2 to give

$$\exp\frac{qV_{oc}}{kT} = (1 + \frac{BL}{I_o}),$$

so that

$$t = \tfrac{1}{2}\left[1 + \exp\frac{q(V_{oc} - V)}{kT}\right].$$

The open-circuit noise temperature ratio, then, is

$$t_{oc} = \tfrac{1}{2}(1 + 1)$$
$$= 1$$

that is, the open-circuit noise of an illuminated ideal diode is, under

these assumptions, that expected from the same impedance in thermal equilibrium. If current flows, however, increased noise may be expected since then $V < V_{oc}$ for a given $\frac{BL}{I_o}$.

Subject to our assumptions, then, we have shown that although an open-circuited illuminated ideal diode exhibits thermal noise only, use of the diode to deliver current to a load (or to accept current from a source) will increase the noise. The effect of current flow within the device will next be considered. This situation could arise in an ideal diode if the illumination were not perfectly uniform. Let us suppose, for example and as a rough approximation, that hole-electron pairs are being created by light uniformly in part of the diode (to which we may thus apply equation 2), but are being produced only thermally in the rest of it (to which we may apply equation 1). Then we may represent the system by two diodes in parallel:

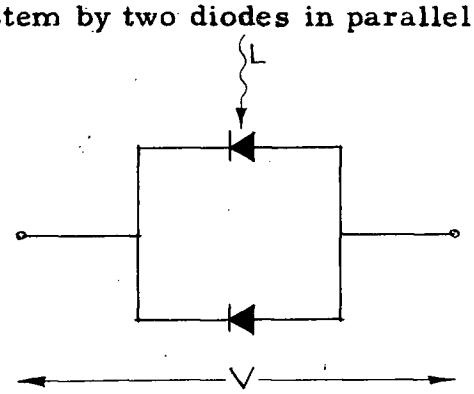

Diode 1: $I_1 = I_{o1}(\exp\frac{qV}{kT} - 1) - BL$

Diode 2: $I_2 = I_{o2}(\exp\frac{qV}{kT} - 1)$

where diodes 1 and 2 represent the illuminated and dark portions respectively of the complete device. We shall also assume the two parts of the diode to be at the same temperature.

Proceeding in the same way as before, we write for the shot noise density

$$\frac{\overline{i_1^2}}{\Delta f} = 2q(I_o \exp\frac{qV}{kT} + I_{o1} + BL)$$

and $$\frac{\overline{i_2^2}}{\Delta f} = 2q(I_{o2}\exp\frac{qV}{kT} + I_{o2}) .$$

Hence $$\frac{\overline{i^2}}{\Delta f} = 2q\left[(I_{o1} + I_{o2})\exp\frac{qV}{kT} + I_{o1} + I_{o2} + BL\right].$$

The total current through the composite diode is

$$I = (I_{o1} + I_{o2})\exp\frac{qV}{kT} - (I_{o1} + I_{o2}) - BL$$

so that its low frequency conductance is

$$G = \frac{\partial I}{\partial V} = \frac{q}{kT}(I_{o1} + I_{o2})\exp\frac{qV}{kT} .$$

Then $$t = \frac{\overline{i^2}}{4kTG}$$

$$= \tfrac{1}{2}\left[1 + (1 + \frac{BL}{I_{o1} + I_{o2}})\exp(-\frac{qV}{kT})\right].$$

Since $I_o = I_{o1} + I_{o2}$, the noise temperature ratio is unchanged by the non-uniformity of the illumination. In particular, in the open-circuit condition

$$\exp\frac{qV_{oc}}{kT} = 1 + \frac{BL}{I_{o1} + I_{o2}}$$

so that $$t_{oc} = 1.$$

Thus the internal current produced in the diode by non-uniform illumination does not cause an addition to the measurable noise. This result simplifies the experimental techniques, since no special attention need be paid to the homogeneity of the incident light beam or to the detailed geometry of the junction.

The objection might reasonably be raised that the hole-electron pairs produced by the light are being created with energies in many cases considerably in excess of the thermal energy of the crystal lattice, and it would seem possible that prior to thermalization these pairs could lead to additional noise. Davydov (Tauc, 1957) has shown, however, that this thermalization takes place in a time very short compared with the lifetimes of the minority carriers: representative figures being 10^{-11} seconds for the thermalization process and 10^{-6} seconds

for a typical lifetime. This is further support for the theory that the noise under illumination should be predicted - at least approximately - by Nyquist's expressions, since the photocarriers will have energies corresponding to the lattice temperature except for a very short initial period of elevated energy.

1.3 Objective of Present Work

The objective of the present work is to provide an experimental basis for a noise generation model which, it is hoped, will predict the open-circuit noise voltage appearing at the terminals of an illuminated photo-diode in terms of the measurable parameters of that diode. In particular, it is proposed to investigate the possibility of predicting this noise voltage on a 'quasi-Nyquist' basis; that is, can the noise of an illuminated device still be ascribed to the Nyquist-predicted thermal noise of the real part of the junction impedance at the same frequency (as the noise measurement is made) and under the same illumination?

To this end, a photo-diode has been selected whose direct current characteristics appear nearly ideal. Various measurements are described from which the parameters characterizing the device can be inferred. These include direct current measurements of short-circuit current and open-circuit voltage under varying illumination, current and voltage under constant illumination, and impedance at frequencies from 1 to 100 kc under varying illumination. The diode's noise has been measured (limited to frequencies from 20 to 30 kc by equipment and techniques available) as a function of illumination and in terms of equivalent noise resistance.

CHAPTER 2 - EXPERIMENTAL INVESTIGATIONS

2.1 Direct Current Characteristics

Photo-diodes available for selection were types 5C and 1N188A grown germanium p-n junctions manufactured by Clevite Transistor Products. The direct current characteristics of two of the former and five of the latter were measured both in the dark and under constant illumination, and one of the former was selected for further investigation because of its near-ideal performance. The experimental setup was as follows:

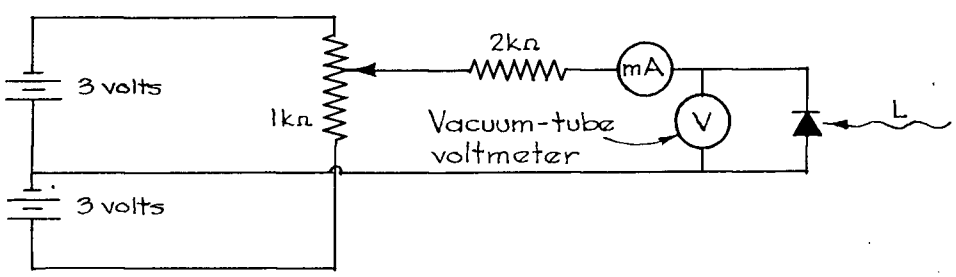

The results of these measurements with the selected diode are those shown in figure 1. The saturation evidenced by the reverse characteristic indicates consistency with equations 1 and 2 for the dark and light characteristics respectively.

Further evidence for the applicability of these equations is obtained by considering the photocharacteristic equation. Examining equation 2 under short-circuit conditions (V = 0) gives

$$I_{sc} = -BL \tag{5}$$

and under open-circuit conditions (I = 0) gives

$$0 = I_o(\exp\frac{qV_{oc}}{kT} - 1) - BL .$$

FIGURE 3

FORWARD DARK, FORWARD ILLUMINATED,

AND PHOTOCHARACTERISTICS

OF SELECTED DIODE

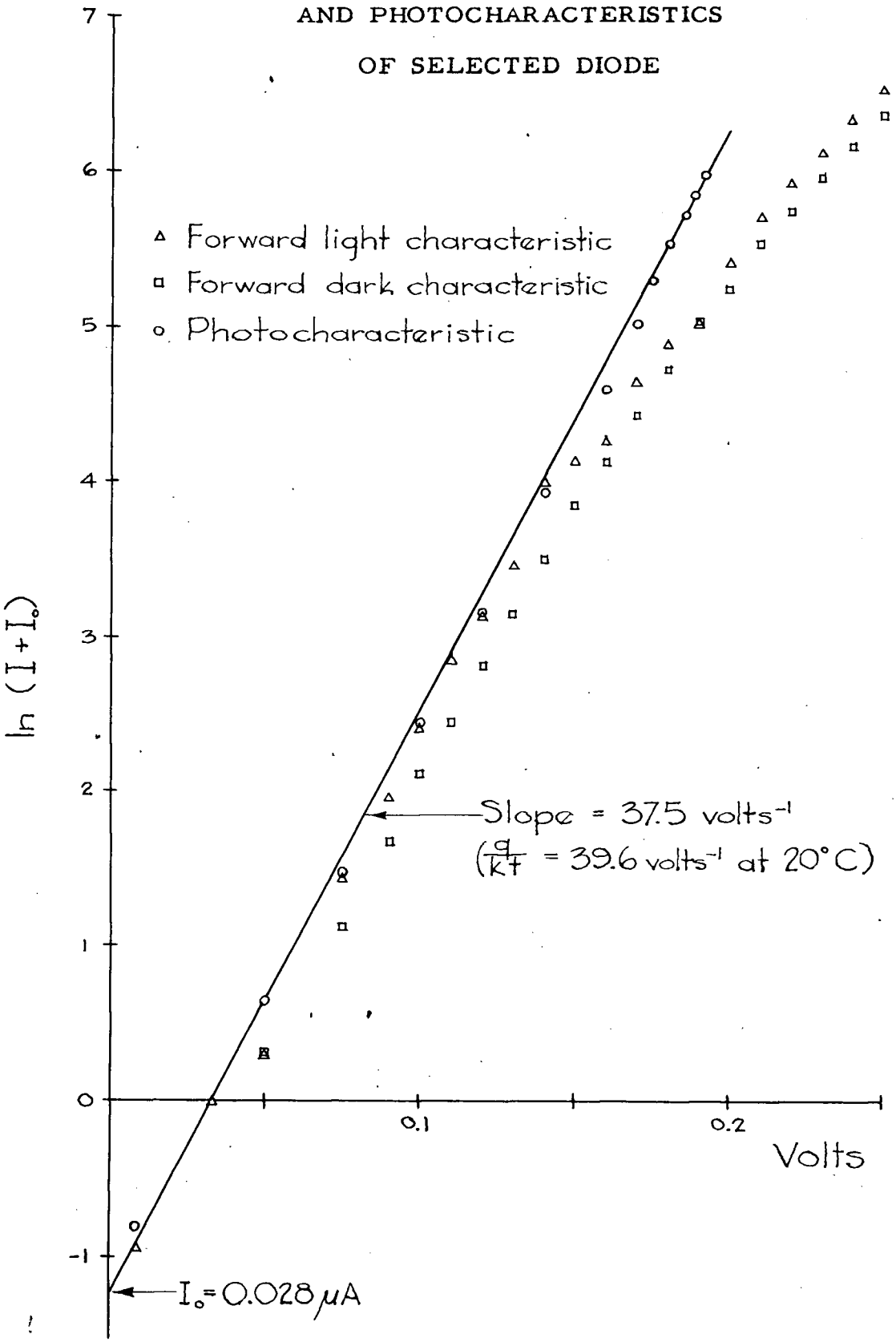

Combining these gives the photocharacteristic equation for the model:

$$|I_{sc}| = I_o(\exp\frac{qV_{oc}}{kT} - 1) \tag{6}$$

or

$$\ln(|I_{sc}| + I_o) = \frac{q}{kT}V_{oc} + \ln(I_o) .$$

This equation is of the same form as the forward dark characteristic. Thus a plot of $\ln(|I_{sc}| + I_o)$ versus V_{oc} should be a straight line of slope $\frac{q}{kT}$ if this model is valid. Figure 3 is such a plot and suggests rather good agreement. It should be noted that the ordinate axis intercept of the line obtained from the high current readings (such that $|I_{sc}| \gg I_o$) gives an approximation to $\ln(I_o)$; using this value for I_o enables the plot of $\ln(|I_{sc}| + I_o)$ to be completed at low currents.

The measurements for the photocharacteristic plot were obtained using a heavily shunted mirror-type galvanometer for I_{sc}, a potentiometer for V_{oc}, and a 150 watt incandescent projection lamp for a light source. Variation of light intensity was provided for by running the lamp from 60 cs power obtained through a variable autotransformer. The optical arrangement consisted of a single converging lens of about 20 cm focal length to concentrate the light somewhat and a block of clear lucite about 1 inch thick to minimize heating effects. The lucite is a good absorber of those wavelengths greater than that corresponding to the energy gap in germanium which would produce only heat in the diode.

The slope of the photocharacteristic line in figure 3 is about 37.5 volt^{-1}, whereas $\frac{q}{kT}$ for room temperature (20°C) is 39.6 volt^{-1}; so the results are in reasonable agreement. The ordinate axis intercept leads to an estimate that I_o is about 0.3μA for this diode. This is of the same order as the reverse saturation current noted. The difference at -2.0 volts bias would lead to a value of β of about 0.005 if the Bethe

FIGURE 4

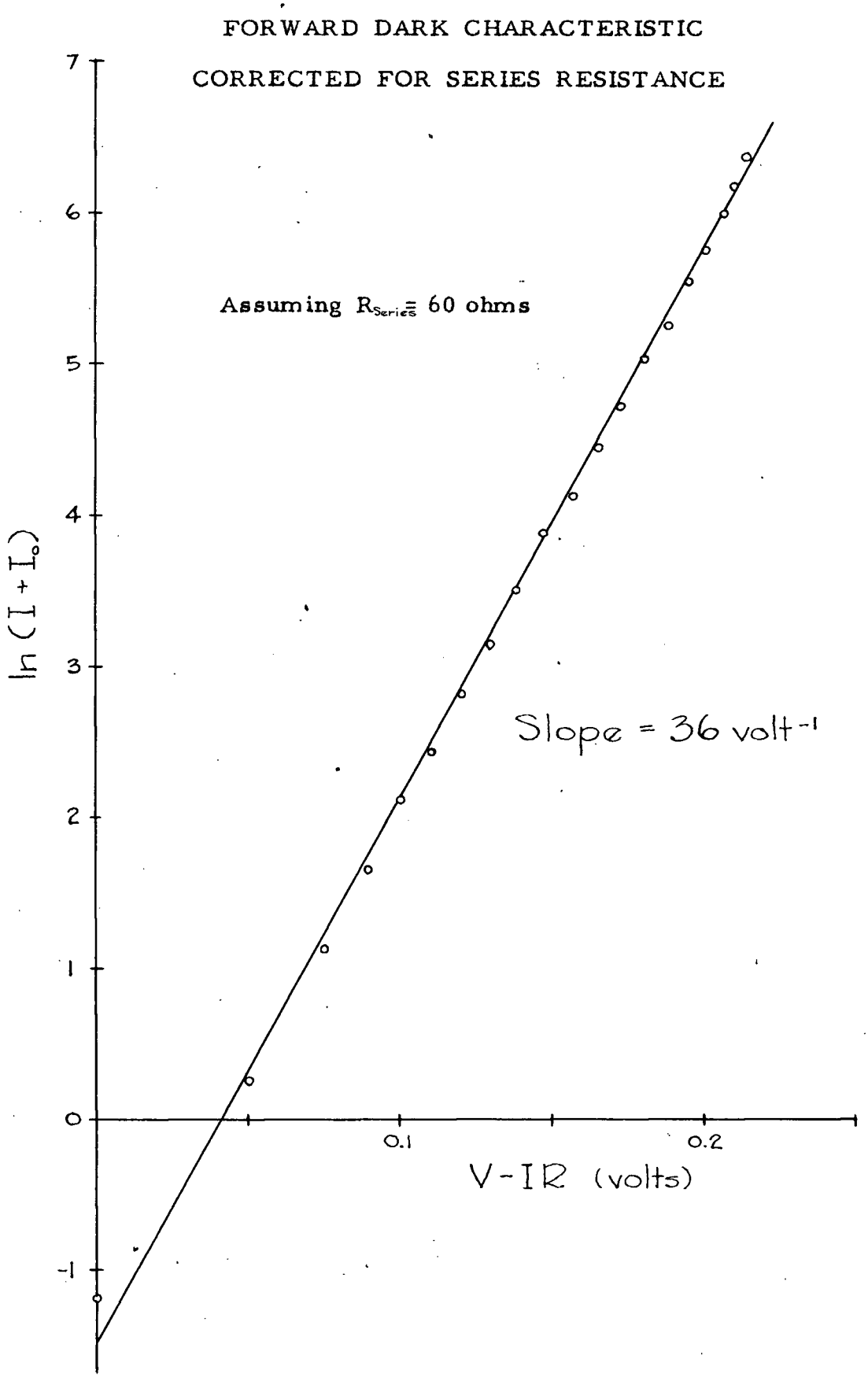
FORWARD DARK CHARACTERISTIC
CORRECTED FOR SERIES RESISTANCE
Assuming $R_{Series} \cong 60$ ohms
Slope = 36 volt^{-1}
ln (I + I$_o$)
V - IR (volts)
7
6
5
4
3
2
1
0
-1
0.1
0.2

expression (page 4) were fitted there. The Bethe equation was thus not considered further.

Figure 3 shows also the data of figure 1 replotted with semilogarithmic co-ordinates (I_{sc} has been added to each illuminated current reading to enable its form to be compared with the others' more easily). In general both these sets of data agree fairly well with the photocharacteristic, although both fall somewhat below it. This behavior can be explained by assuming the existence of series resistance within the diode. Consider the simple equivalent circuit:

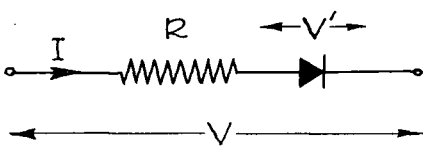

Although V' is clearly the quantity used in the basic diode equations, V is the quantity actually measured. However $V' = V - IR$ so we may rewrite equation 1 in terms of the measurable voltage V as

$$I = I_o \exp\left[\frac{q(V - IR)}{kT}\right] - I_o$$

and for the purposes of figure 3 as

$$\ln(|I| + I_o) = \frac{q}{kT}(V - IR) + \ln(I_o) .$$

Substituting the known and previously calculated values and using an experimental point which appears representative of the forward dark line (point at 0. 2 volt) indicates that the curvature of figure 3 is consistent with a series resistance somewhat greater than 50 ohms. The forward dark characteristic corrected on the assumption of 60 ohms series resistance is plotted in figure 4. The linearity improvement made by this correction is quite apparent. The slope of the line shown is about 36 volt^{-1} compared with $\frac{q}{kT} = 39.6$ volt^{-1}.

The fact that the slopes of the lines plotted (particularly the last-mentioned) are not quite equal to $\frac{q}{kT}$ may indicate a departure from the behavior predicted by Shockley, although not necessarily a departure from general ideal behavior, of which Shockley's model is a special case (for small injected carrier densities). This point will be discussed in connection with the interpretation of certain of the alternating current measurements.

No attempt was made in these or later experiments to measure the absolute magnitude of the light intensity incident on the junction. Such factors as cell orientation and junction geometry would make this measurement of little meaning in any case. The significant quantity, in the light of the previously derived relation

$$I_{sc} = -BL \tag{5}$$

is the short-circuit current through the diode. This is always a measure of the rate of production of photo-electron-hole pairs, and avoids all difficulties involved in measuring the spectral distribution of the light and in considering the internal structure of the device.

2.2 Alternating Current Measurements

Following the success in relating the direct current characteristics to a simple model, it was hoped that the alternating current behavior could in some fashion also be explained in terms of a simple picture. A reasonable equivalent circuit for a real diode at some fixed bias is:

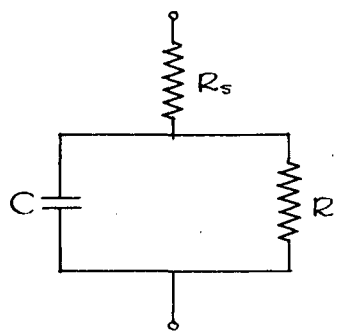

where R and C make up the junction impedance and geometric shunt capacitance of the device and R_s represents the bulk resistance of the semiconductor together with contact and lead resistances. Suppose we measure this admittance (still at a fixed bias) as a function of frequency and in terms of its parallel components. Then

$$Y = \frac{1}{Z} = \frac{1 + j\omega CR}{R + R_s(1 + j\omega CR)}$$

$$= \frac{R + R_s + \omega^2 C^2 R R_s + j\omega CR^2}{(R_s + R)^2 + (\omega CRR_s)^2}$$

$$= \frac{1}{R_s} - \frac{R}{R_s}\left[\frac{(R_s + R)}{(R_s + R)^2 + (\omega CRR_s)^2}\right] + \frac{j\omega CR^2}{(R_s + R)^2 + (\omega CRR_s)^2}.$$

Then if we adopt the notation

$$Y = G + jS$$

we may identify $$G = \frac{1}{R_s} - \frac{R}{R_s}\left[\frac{(R_s + R)}{(R_s + R)^2 + (\omega CRR_s)^2}\right]$$

and $$S = \frac{\omega CR^2}{(R_s + R)^2 + (\omega CRR_s)^2}.$$

If we now let $R_m = \frac{1}{G}$ and C_m be the parallel components actually measured,

FIGURE 5

EXPERIMENTAL ARRANGEMENT FOR MEASUREMENT OF DARK AC ADMITTANCE

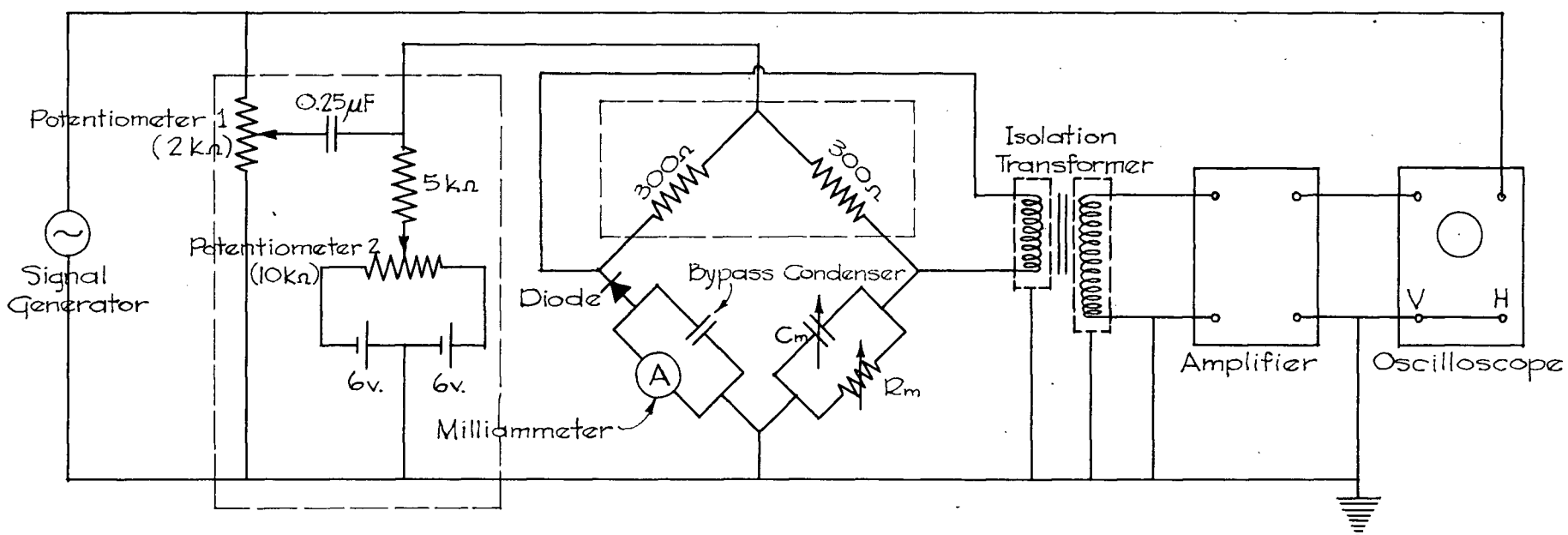

we see that $S = \omega C_m$

and therefore $(R_s + R)^2 + (\omega C R R_s)^2 = \frac{CR^2}{C_m}$.

Substitution of this into the expression for G gives

$$\frac{1}{R_m} = G = \frac{1}{R_s} - \frac{(R_s + R)}{CRR_s} C_m .$$

Hence if we plot the measured conductance G (the reciprocal of the measured parallel resistance component of the admittance) against the measured parallel capacitance, we should obtain a straight line intersecting the ordinate axis at $\frac{1}{R_s}$. This line is generated by varying the frequency of measurement.

The experimental arrangement for the dark admittance measurement is shown in figure 5. Potentiometer 1 is used to set the ac signal level across the diode to a sufficiently low level to avoid displacement of the operating voltage (at the measured current) and excessive harmonic distortion due to the diode's non-linearity. Potentiometer 2 is used to set the bias level. Bias current rather than voltage is measured since it is generally the more sensitive parameter. The output isolation transformer is oriented for minimum 60 cs magnetic pickup from the many sources in the laboratory. Final balance, obtained by adjustment of the R_m and C_m elements, is displayed as an elliptical pattern on an oscilloscope to discriminate against harmonics, noise, and hum.

To check the operation of the bridge, a dummy diode was prepared as a test circuit. It consisted of a 0.06 μF capacitor and a 470 ohm resistor in parallel representing the junction impedance, both in series with a 100 ohm resistor representing the series resistance. The admittance of this dummy was measured from 5 to 100 kc and the

FIGURE 6

MEASURED CONDUCTANCE VERSUS
MEASURED PARALLEL CAPACITANCE
FOR DUMMY AND REAL DIODE

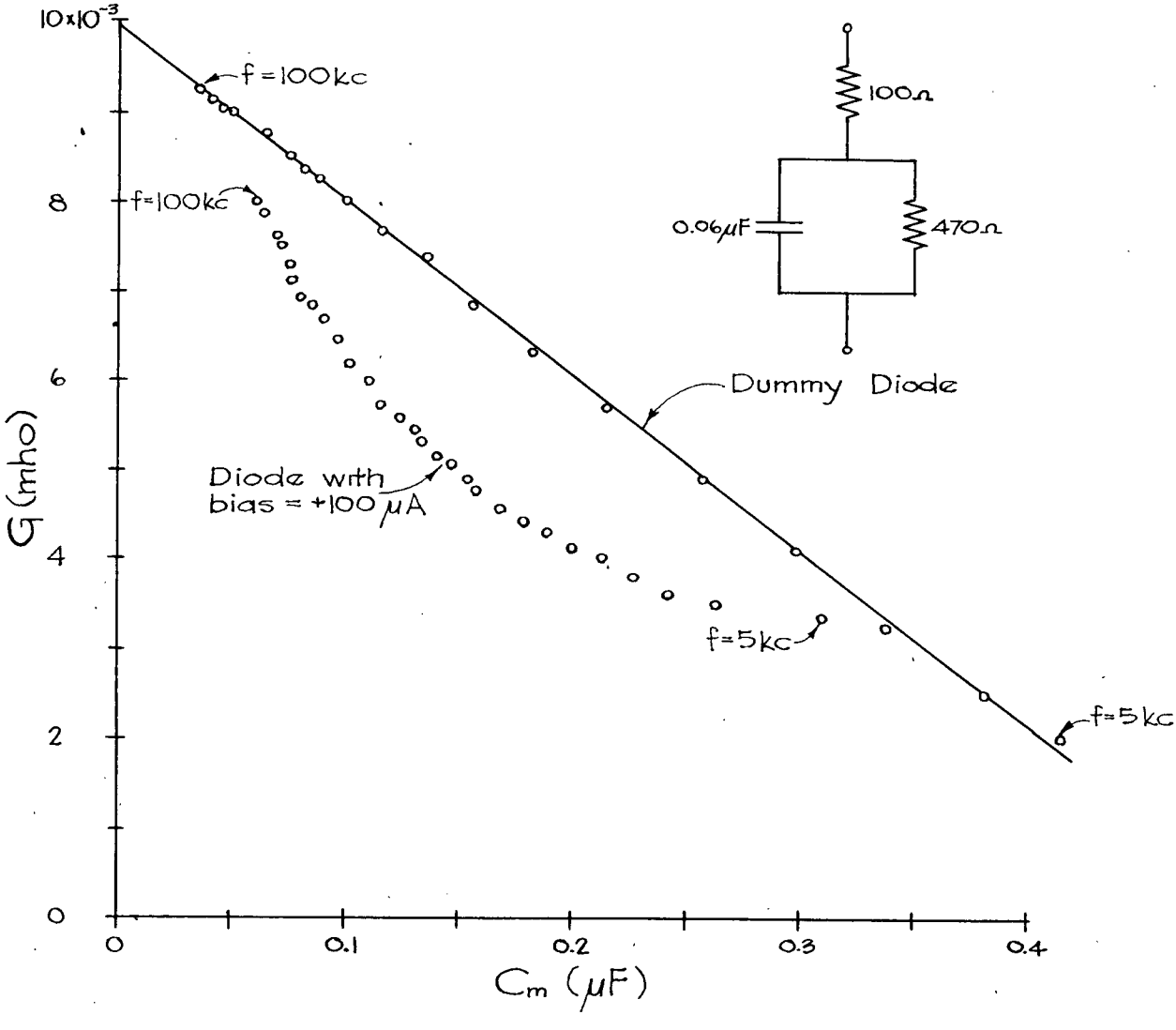

results plotted as suggested above - see figure 6. The ordinate axis intercept of the best straight line through the points confirms exactly (within the limit of accuracy of the graph) the value of series resistance used.

Also plotted on this graph is a typical set of points obtained from measurement of the dark diode admittance under forward bias. The pronounced curvature evident here was noted at all biases investigated (+20 to +150 μA). It may therefore be concluded that the simple equivalent circuit suggested cannot be applied to the device.

This method also eliminates from consideration the two slightly more complicated resistance-capacitance networks depicted below:

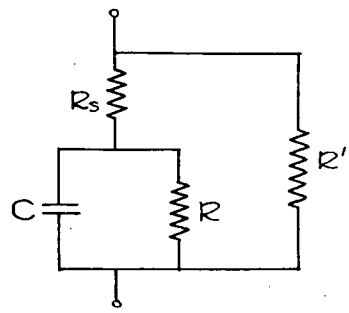

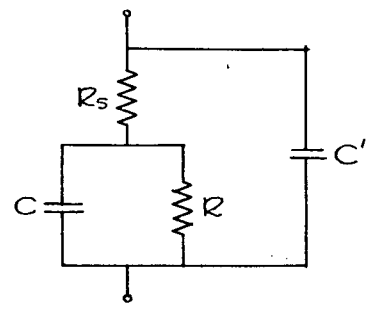

The first of these leads to a straight line displaced vertically from that of the simple case by the added shunt conductance $\frac{1}{R'}$, while the second leads to a straight line displaced horizontally by the added capacitance C'. Neither of these networks, therefore, are applicable as equivalent circuits.

Since we hope to relate measured diode noise to measured diode conductance, the lack of a simple model on which to base the latter is regrettable but by no means serious. Because the diode admittance can readily be measured under conditions to be encountered, no further effort was directed to finding a model by which it might be predicted.

FIGURE 7

EXPERIMENTAL ARRANGEMENT FOR MEASUREMENT OF ILLUMINATED AC ADMITTANCE IN OPEN-CIRCUIT CONDITION

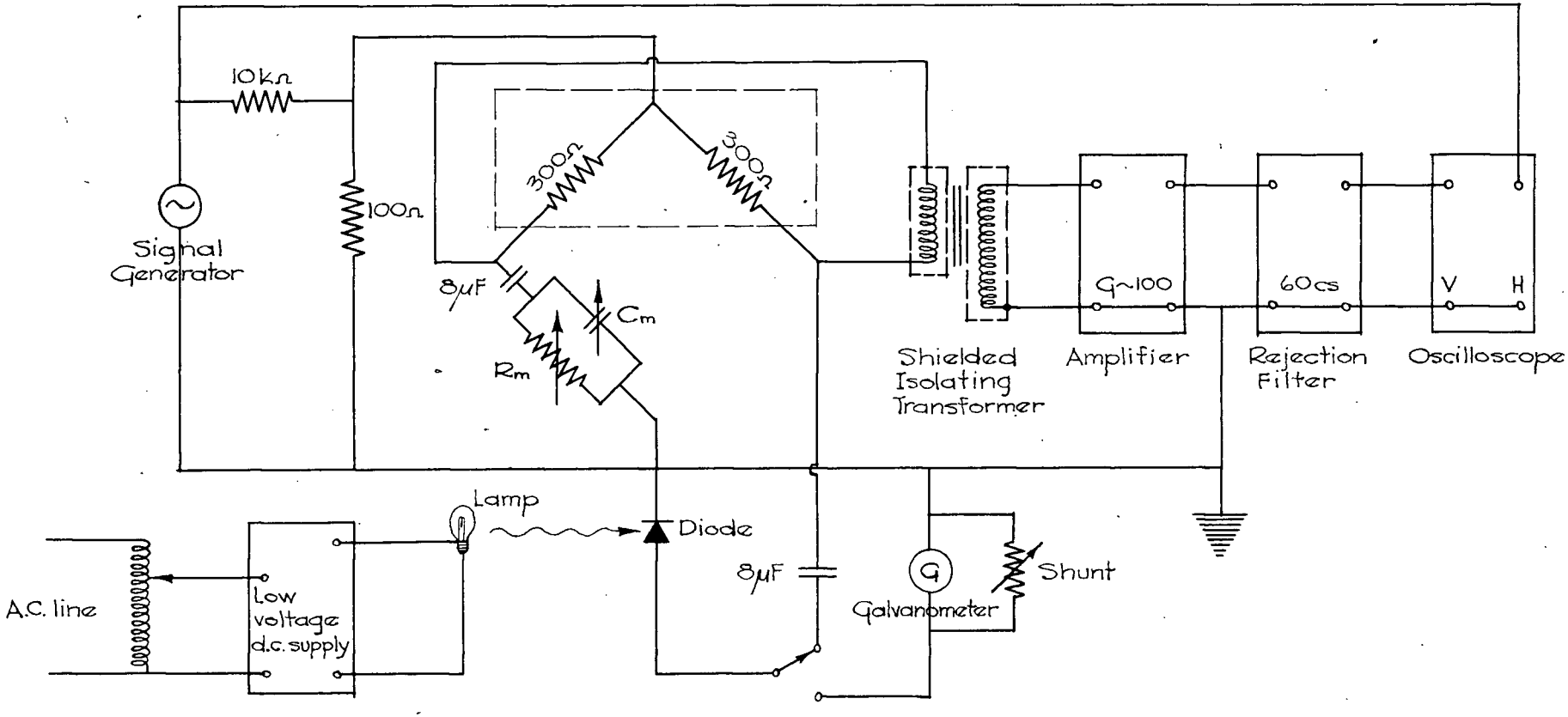

The measurement of diode admittance under illumination is undertaken in very much the same manner. The effective illumination at the junction is determined by measuring the diode's short-circuit current (see equation 5). Then the device is switched into the bridge circuit in series with a large capacitance to ensure open-circuit conditions. A similar capacitance in the variable arm of the bridge minimizes error due to the added element.

The requirement of open-circuit measurement, however, introduces an interesting complication. The rest of the bridge may be considered to be an alternating current source, so the diode-capacitor system may be thought of as a rectifier-filter combination:

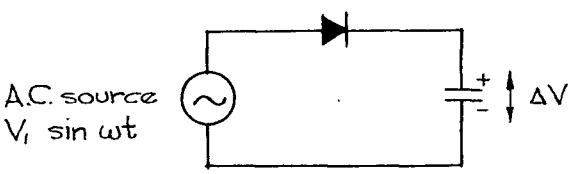

A net dc bias will therefore appear across the diode in these circumstances even without illumination. Hence the photo-bias supposedly set by adjusting the illumination for a given short-circuit current will be disturbed when alternating current from the bridge is applied. It is shown in the appendix that this additional bias (ΔV) is given by

$$\Delta V = -\frac{qV_1^2}{4kT}$$

where $V_1 \sin \omega t$ is the applied ac voltage. It is interesting to note that this bias shift is independent of the level of illumination.

The effect of this shift in dc bias is also investigated in the appendix and it is shown that the error in the measured conductance

FIGURE 8

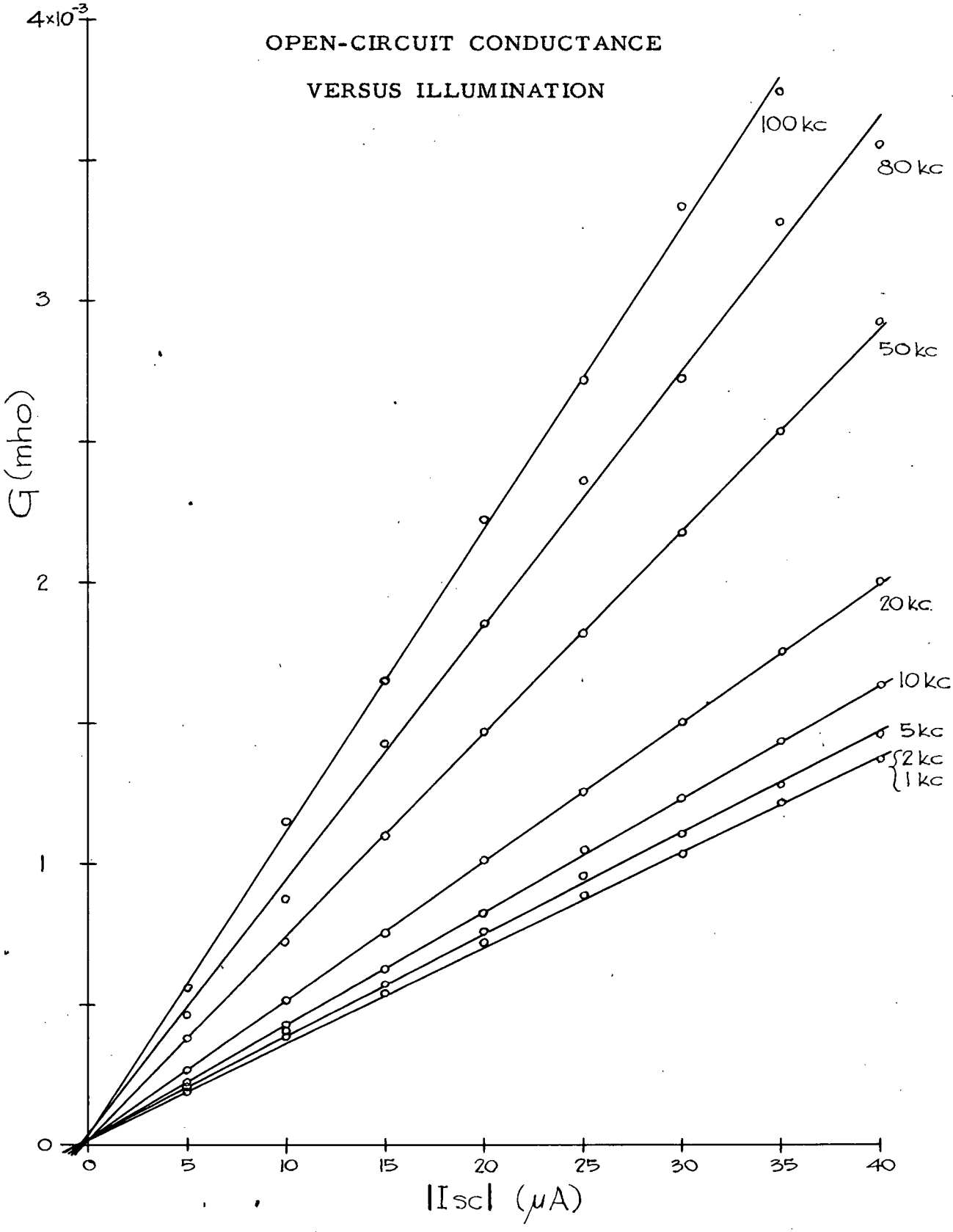
OPEN-CIRCUIT CONDUCTANCE
VERSUS ILLUMINATION
4×10⁻³
3
2
1
0
G (mho)
100 kc
80 kc
50 kc
20 kc
10 kc
5 kc
2 kc
1 kc
0
5
10
15
20
25
30
35
40
|Isc| (μA)

from this cause will be less than 1% if V_1 is less than about 5 mv. For this reason the signal generator output is kept as low and the detector sensitivity raised as high as practicable (limited by noise and hum) so that the ac signal across the diode can be kept sufficiently low. Illumination is provided by a low-voltage lamp run from a variable dc supply to avoid ripple fluctuations in the light intensity. The experimental arrangement is shown in figure 7.

Since we are now to be concerned with frequency-dependent quantities, we shall designate the diode conductance by the symbol $G(\omega)$ and thus its low frequency value (G in earlier sections) by $G(0)$. The open-circuit low frequency conductance (which we shall call $G_o(0)$) is obtained from equation 3 (page 8) by setting $I = 0$. Thus:

$$G_o(0) = \frac{qI_o}{kT} \exp \frac{qV_{oc}}{kT}$$

$$= \frac{q}{kT}(I_o + |I_{sc}|).$$

Therefore successive plots of $G_o(\omega)$ versus the short-circuit current should approach, as the frequency is decreased, a straight line of slope $\frac{q}{kT}$ and abscissa axis intercept $-I_o$. Figure 8 is such a plot.

Since the 1 and 2 kc plots on this graph are virtually indistinguishable, their slope should be a good approximation to the zero frequency value. The slope of the 1 kc line shown in figure 8 is about 35 volt^{-1}, compared with the calculated value for $\frac{q}{kT}$ of 39.6 volt^{-1} at room temperature. It might be noted, however, that the value found is in good agreement with the value of 36 volt^{-1} obtained from consideration of the forward dark characteristic (page 15).

The scales of the quantities plotted in figure 8 make any accurate estimate of I_o from the axis crossing quite impossible. The

FIGURE 9

VARIATION OF CONDUCTANCE WITH FREQUENCY

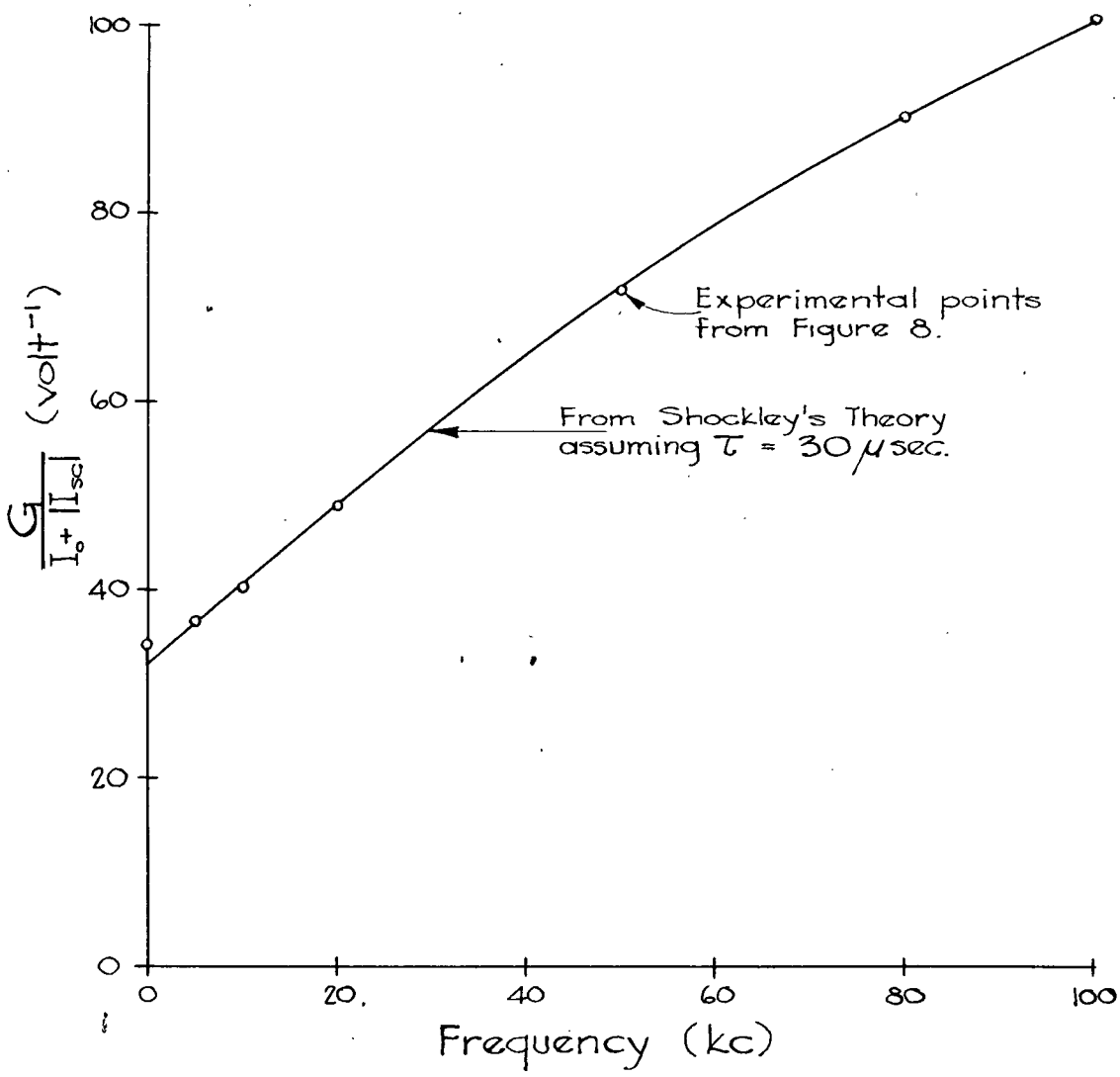

figure does, nevertheless, suggest our previous estimate of 0.3μA is not at all unreasonable.

The variation with frequency of the diode's conductance makes possible a check on the applicability of Shockley's carrier diffusion theory and, should this theory be valid, permits an estimate of the minority carrier lifetime τ. Shockley's theory predicts that

$$Y(\omega) = G(0)(1 + j\omega\tau)^{1/2}.$$

Therefore

$$G_o(\omega) = G_o(0)\mathrm{Re}(1 + j\omega\tau)^{1/2}$$

$$= G_o(0)\left[\frac{1 + \sqrt{1 + \omega^2\tau^2}}{2}\right]^{1/2} \qquad (6)$$

at any fixed bias or level of illumination (which determine $G_o(0)$).

Now $G_o(\omega)$ is a function both of frequency and of illumination (as measured by I_{sc}). We have shown that for low frequencies, however, $\frac{G_o(0)}{I_o + |I_{sc}|}$ is a constant independent of illumination (theoretically equal to $\frac{q}{kT}$), and figure 8 indicates that at higher frequencies this proportionality is maintained, although the proportionality constant is a function of frequency.

Shockley's theory may be used to predict the variation of this proportionality constant (which is, at a given frequency, the slope of the appropriate line in figure 8) by dividing both sides of equation 6 by $(I_o + |I_{sc}|)$. Therefore:

$$\frac{G_o(\omega)}{I_o + |I_{sc}|} = \frac{G_o(0)}{I_o + |I_{sc}|}\left[\frac{1 + \sqrt{1 + \omega^2\tau^2}}{2}\right]^{1/2}$$

The values of the slopes of the lines in figure 8 are plotted against frequency in figure 9, as is a line derived from Shockley's theory assuming a τ of 30μsec.

Using this value for the lifetime, the correction term in equation 6 is about 1.005 at 1 kc, indicating that the 1 kc measurements

are a good approximation to the zero frequency characteristics. The value of $\omega\tau$ itself varies from about 0.2 at 1 kc to about 20 at 100 kc. The good agreement between experiment and Shockley's theory over this wide range of $\omega\tau$ is strong evidence in favour of its applicability.

Thus the alternating current measurements lend confirmation to the validity of Shockley's diffusion theory applied to this case, and also indicate that the low frequency behavior of the diode ($\omega\tau \ll 1$) can be predicted by differentiation of equation 2 under the appropriate conditions. The measured slope of the low frequency conductance versus short-circuit current (figure 8) does not agree with the theoretically predicted value of $\frac{q}{kT}$. This result confirms the indications in certain of the dc measurements (page 16) that the diode is in some respect non-ideal.

2.3 Noise Measurements

The measurement of noise within some bandwidth involves, essentially, selection of that pass band by a suitable filter and detection of the average signal therein by a suitable detector. In practice, small noise signals must be amplified (before or after frequency selection) and hence some method must be available by which the noise of interest may be recognized against the background of amplifier noise. In general, this means that the amplifier noise will limit the resolution of the source noise measurements by completely overshadowing very small changes.

The average signal voltage to be expected after detection is a function of the bandwidth in which it is measured; being strictly proportional if the detector follows a square law and if the noise is white, i.e. constant in mean square value with respect to frequency, as is thermal noise. The variance of the detected output will vary in some inverse fashion with the bandwidth so that the wider the bandwidth the larger and more nearly constant will be the detected signal.

Filtering may be employed to reduce variations in the output signal, but it must be used with care if there is any spurious interference present in or picked up by the measuring set, since long time-constant filtering will smooth these out and add their contributions to the recorded level with no indication of their transient nature.

Several factors govern the choice of measurement frequency. To measure what might be called junction noise as opposed to excess surface-dependent noise, low frequencies should be avoided. On the other hand, measurement at high frequencies is made difficult

by the effect of shunt capacitance in the amplifier input circuit.

Equipment available for filtering and detection included a General Radio type 736-A wave analyzer covering 20 cs to 16 kc with a bandwidth of about 4 cs, and a Sierra type 121 analyzer covering 15 to 500 kc with a bandwidth of about 200 cs. Additional filtering was added to the detector stages of both analyzers in order to reduce the fluctuations of output voltage.

Because of its much narrower sampling band, the lower frequency analyzer required a much longer time-constant filter following the detector to reduce these fluctuations to a useful degree. However, intermittent and probably random interference from fluorescent lamp starters and electric motors in the vicinity was noted at a mean rate comparable with the reciprocal of this necessary time constant. These interfering bursts were, therefore, averaged along with the noise recorded by this analyzer. The shorter time constant needed for reasonable results with the higher frequency analyzer left the interference almost intact (that is, it appeared still as bursts at the detector-filter output) so it could be ignored when interpreting the results. For this reason the Sierra equipment was used exclusively. The adverse effect of input shunt capacitance at higher frequencies indicated that the lower part of this instrument's range would give the most accurate measurements. These measurements were, therefore, made at 20 and 30 kc.

The wave analyzer itself has insufficient gain to enable diode noise to be measured directly, so two preamplifiers are cascaded ahead of it. The first of these is a single tube amplifier with a voltage gain of about 2.6 which is designed with as low an input capacitance as

. FIGURE 10

USE OF RESISTANCE BOX THERMAL NOISE
TO DETERMINE NOISE BANDWIDTH
OF ANALYZER

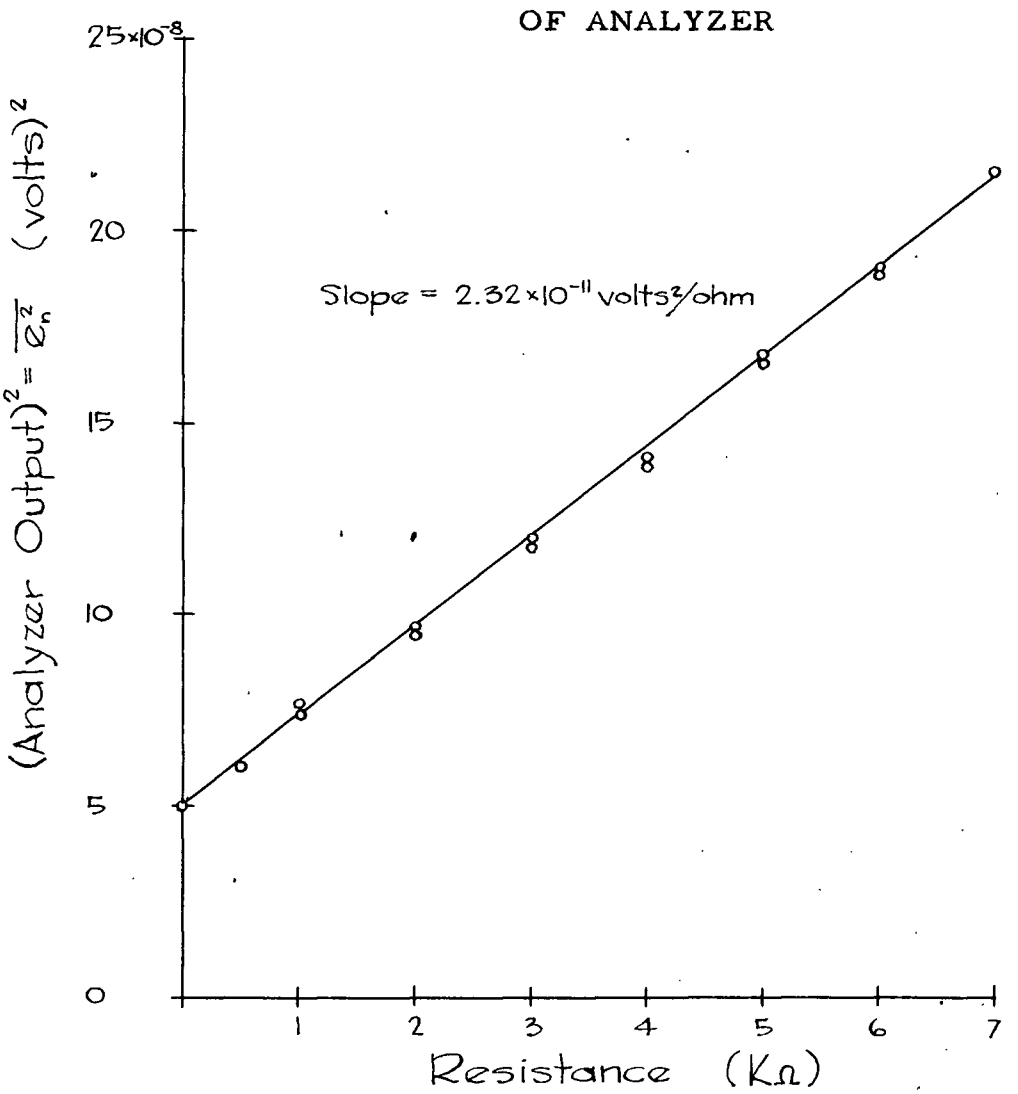

practicable. Its gain varies slowly with time over a range of about ±10%. The second unit is a Technology decade amplifier with a stabilized gain of 1000. The power inputs to both units are regulated.

Because of the variation in detector output, whose modified filter system has a time constant of about 0.8 seconds, the output is permanently recorded as a function of time on a self-balancing recording potentiometer. Examination of the record from this instrument over a sampling time of a minute enables a good estimate to be made of the average reading and also reveals any marked gain drift in any of the equipment.

As a test of the noise measuring set and of measurement techniques, the noise output of a resistance box was measured. The box consists of wire-wound resistors which should be quite free of any but thermal noise. In any case, the box was measured under open-circuit conditions and so could not generate any current-dependent noise. The results of one such trial (20 kc) are shown in figure 10.

Now $\overline{e^2} = 4kTR\Delta f$

and therefore $\Delta f = \dfrac{\overline{e^2}}{4kTR}$.

But $\dfrac{\overline{e^2}}{R}$ is the slope of the line drawn in figure 10 corrected for the gain of the amplifier (2580 in this case), so that

$$\frac{\overline{e^2}}{R} = \frac{2.32 \times 10^{-11}}{(2580)^2} \text{ volt}^2/\text{ohm},$$

and thus $\Delta f = 210 \text{ sec}^{-1}$.

This value is in good agreement with the value of ±100 cs (to -3db points) specified by the manufacturer. The magnitude of the point scatter reflected onto the R axis suggests that the precision of measurement corresponds to about 200 ohms.

When the dc power to the illuminating lamp is interrupted the light output falls off with a measured decay time of about 0.3 seconds. This indicates that the thermal inertia of the lamp will prohibit illumination fluctuations occurring at frequencies higher than several cycles per second ($\omega\tau$ for the lamp is greater than 1 for $f > 0.5$ cs) so that no photovoltaic noise should be introduced directly by fluctuations of the light intensity in the frequency range of interest.

It is to be expected that the various amplifier gains (except, perhaps, that of the decade amplifier) and the bandwidth of the wave analyzer will drift over a period of time. This makes a substitution technique for noise measurement particularly desirable, since with such a method the measurement is strictly comparative and is independent of the absolute values of gain and bandwidth involved. Its success depends on the substitution being made in a time short compared to any drift time, but this criterion can be met.

The choice of a noise standard for substitution is easily made in this case. A saturated noise diode is prone to develop flicker noise, it requires carefully filtered power supplies, and it depends on an external meter for accuracy. A resistance box, on the other hand, requires only shielding and, assuming wire-wound resistors and low-noise switches, represents a very stable and accurate thermal noise source since both the values of resistance and absolute temperature may readily be known to a few parts in 10^3. At high frequencies the shunt capacitance of the decade box will vary according to the decade switches in use, but this difficulty was not encountered to any marked degree throughout this investigation.

FIGURE 11

COMPOSITE EXPERIMENTAL ARRANGEMENT
FOR NOISE AND ADMITTANCE MEASUREMENT
UNDER ILLUMINATION

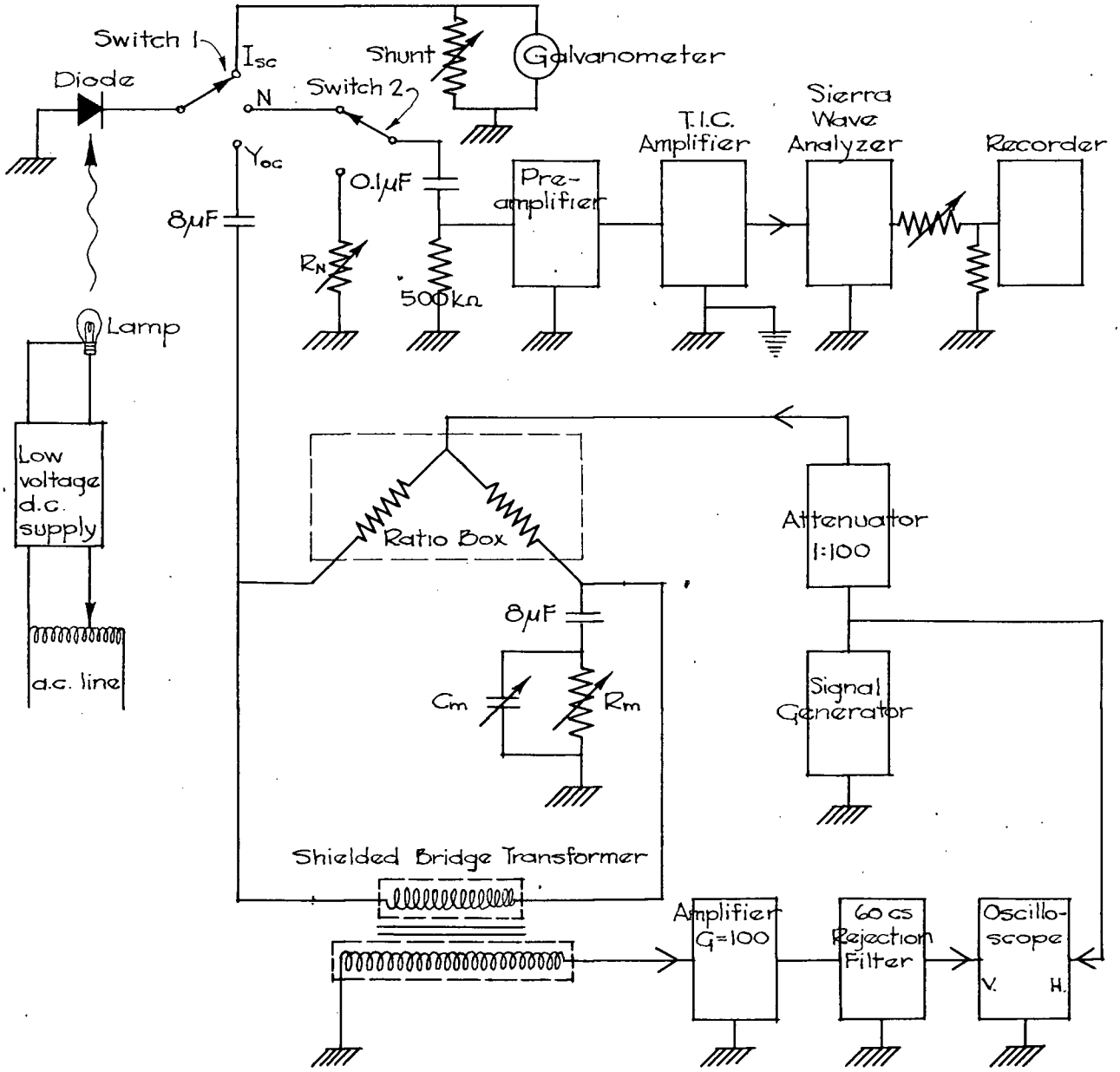

Once again the effective illumination at the junction is measured in terms of the short-circuit current. To avoid the effect of error between the illumination levels set for these noise measurements and those used for the ac admittance measurements, the admittance is measured again directly following the noise measurement and thus under nearly exactly similar conditions.

The composite experimental arrangement is shown in figure 11 and the experimental procedure is as follows:

1. The wave analyzer is set to the appropriate frequency and, with switch 1 in the I_{sc} position, the light intensity is set appropriately by observation of the magnitude of I_{sc}.
2. The signal generator is set to the wave analyzer frequency (there is sufficient leakage between the circuits that a direct connection is unnecessary for this adjustment), switch 1 placed in the Y_{oc} position, and the bridge balanced with the R_m and C_m elements by observing the elliptical pattern on the oscilloscope.
3. The signal generator is turned off (to prevent interference), switch 1 turned to the N position and, with switch 2 as shown in figure 11, a recording is made of the wave analyzer output.
4. Switch 2 is thrown to place the standard resistance box R_N in the noise set input circuit and the value of R_N is adjusted to bring the recorder to the same average balance position as did the diode's noise. R_N, R_m, and C_m are recorded.

Now the effective noise temperature ratio

$$t = \frac{\overline{e_N^2}}{4kTR\,\Delta f}$$

where R is the real part of the junction impedance under the conditions of

FIGURE 12

NOISE TEMPERATURE RATIO

VERSUS ILLUMINATION

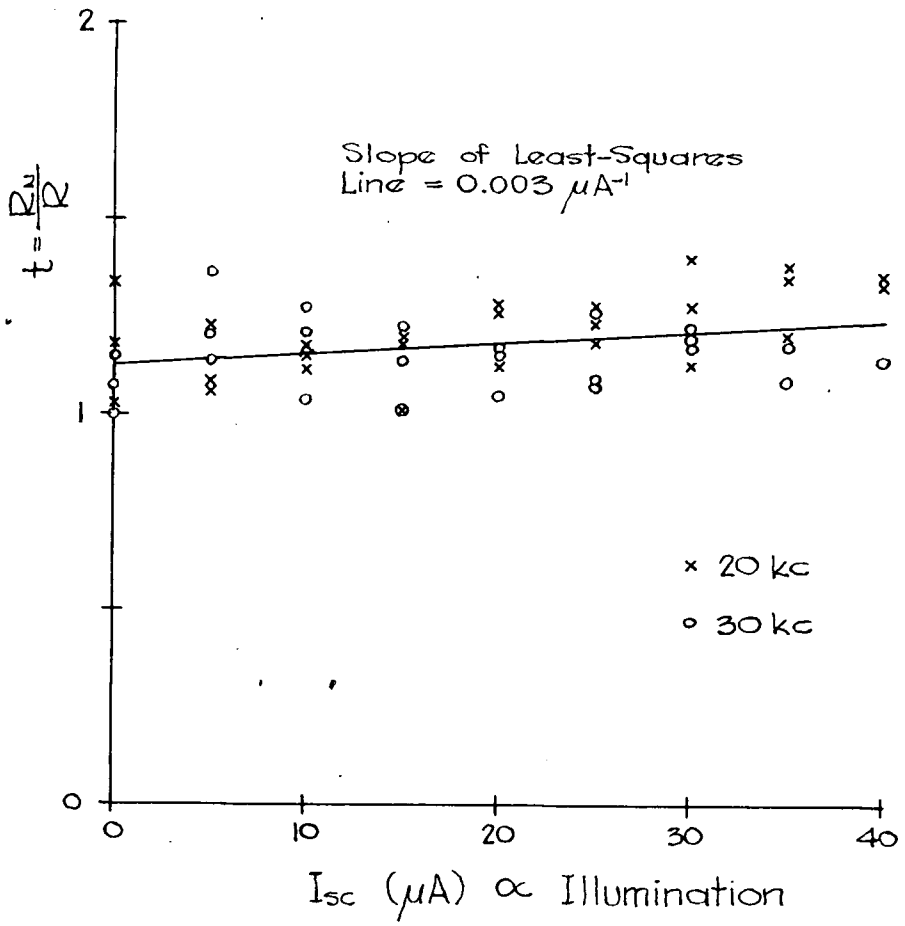

measurement, and $\overline{e_N^2}$ is the measured mean squared noise voltage.

But $$\overline{e_N^2} = 4kTR_N\Delta f ,$$

and hence $$t = \frac{R_N}{R} = \frac{R_N}{R_m}(1 + \omega^2 C_m^2 R_m^2) .$$

The results of the various measurements made are shown in figure 12.

It is difficult to arrive at an accurate estimate of the possible error in the values for t because of the many factors involved. However, R_m can be measured with the bridge described to within 3% and C_m to within 5% or 50 pF, whichever is greater. R_N can generally be estimated to within 10%. Coupled with these errors are several more subtle ones; namely, inaccuracy in the value used for the frequency (which appears in the final expression for t above), drift in illumination, gain, and bandwidth between the various phases of one measurement, and occasional pick-up of aperiodic interference by the noise set (such interference was sometimes observable on an oscilloscope monitoring the input to the wave analyzer). A reasonable estimate of the total possible error in t taking these factors into account would be about ±15%. This figure is in reasonable agreement with the point scatter evident in figure 12.

CHAPTER 3 - DISCUSSION OF RESULTS

3.1 Inferences from DC and AC Measurements

Both the dc and the ac measurements indicate a slight departure in the diode characteristics from those predicted by Shockley. Specifically, his model predicts a current dependence on voltage of the form $(\exp\frac{qV}{kT} - 1)$, which leads also to the low frequency open-circuit conductance dependence (page 21)

$$G_d(0) = \frac{q}{kT}(I_o + |I_{sc}|).$$

Our measurements confirm the general forms of both expressions (that is, in the forward direction the current-voltage relationship is found to be exponential and the open-circuit low frequency conductance is proportional to the illumination and thus to the short-circuit current), but they indicate that Shockley's constant $\frac{q}{kT}$ in either case should be replaced empirically by a somewhat smaller value; about $0.95\frac{q}{kT}$ for the photocharacteristic plot, $0.91\frac{q}{kT}$ for the corrected forward dark characteristic plot, and $0.89\frac{q}{kT}$ for the low frequency conductance plot.

This discrepancy is evidence that Shockley's assumptions are not entirely valid in this case. In particular, his result follows from the result that the hole concentration at the n side of the junction transition region $p(x_{Tn})$ is given by

$$p(x_{Tn}) = p_n \exp\frac{qV}{kT} \tag{7}$$

where p_n is the equilibrium concentration of holes in the n region (and thus also at this plane) and V is the voltage across the junction. Used as a boundary condition for Shockley's solution of the continuity equation in the n region, this expression leads to a diffusion hole current proportional to $(\exp\frac{qV}{kT} - 1)$. A similar treatment of electron current

has a similar result, so that the total current across the junction should be proportional to $(\exp\frac{qV}{kT} - 1)$.

Misawa (1955), however, points out that the hole concentration in question is actually given by

$$p(x_{T_n})\left[p(x_{T_n}) + n_n - p_n\right] = n_i^2 \exp\frac{qV}{kT}$$

where n_n is the equilibrium concentration of electrons in the n region. If the injected carrier density is small (as in Shockley's treatment), $p(x_{T_n}) - p_n$ is very small compared with n_n, and the equation reduces to

$$p(x_{T_n}) = \frac{n_i^2}{n_n}\exp\frac{qV}{kT} = p_n \exp\frac{qV}{kT} .$$

Thus Shockley's result may be seen to be a special case of Misawa's equation.

For the limiting case of high level carrier injection, though, $p(x_{T_n})$ will be very much greater than $n_n - p_n$ and the equation becomes

$$\left[p(x_{T_n})\right]^2 = n_i^2 \exp\frac{qV}{kT}$$

or

$$p(x_{T_n}) = n_i \exp\frac{qV}{2kT} \tag{8}$$

Thus when the injected carrier density is high, this equation leads to a current proportional to $\exp\frac{qV}{2kT}$. Since we found a proportionality roughly to $\exp 0.9\frac{qV}{kT}$ we can assume our conditions fall between the two extremes, but are much more nearly those upon which Shockley's deductions are based. In other words, the junction voltage range we have covered is that for which the characteristics are changing from those of the low-level to those of the high-level case. The change-over is evidently sufficiently gradual that our straight line (figure 4) is a good approximation to what must actually be a curve.

The condition for the onset of high-level injection in the forward direction of a p-n junction is obtained by considering the state

when the hole density at the n-side of the transition region is just equal to the equilibrium electron density, that is;

$$p(x_{Tn}) = n_n.$$

In this case $p(x_{Tn})$ is given by either the low level (equation 7) or the high level (equation 8) formulae above:

$$p(x_{Tn}) = n_n = n_i \exp\frac{qV}{2kT}$$

$$= p_n \exp\frac{qV}{kT}$$

since $\qquad p_n n_n = n_i$.

Solving for the voltage V_o at which this change-over takes place we see:

$$V_o = \frac{2kT}{q} \ln\frac{n_n}{n_i} = \frac{kT}{q} \ln\frac{n_n}{p_n}.$$

In 5 ohm-centimeter material at room temperature the following are representative approximate values for the various concentrations:

$$n_n = 4.2 \times 10^{14}\ \mathrm{cm}^{-3}$$

$$n_i = 2.5 \times 10^{13}\ \mathrm{cm}^{-3}$$

$$p_n = 1.5 \times 10^{12}\ \mathrm{cm}^{-3}$$

These values predict a change-over voltage of about 0.14 volt; a value within, but toward the upper end of, the voltage range investigated experimentally.

Thus the dc and ac measurements suggest that the diode investigated is nearly ideal, although over the range of forward voltage investigated (up to 0.22 volt or about $9\frac{kT}{q}$ across the junction) low injected carrier density characteristics (i.e. Shockley characteristics) are being departed from. They also indicate that the low frequency ac behavior is adequately predicted by differentiation of the dc current-voltage characteristic. Although no simple ac equivalent circuit for the

device is suggested, justification is found for the application of Shockley's carrier diffusion theory to a prediction of the variation of conductance with frequency over a wide (100:1) range of frequency.

3.2 Implications of Noise Measurements

The experimental results for the noise temperature ratio t as a function of illumination in terms of the short-circuit current I_{sc} are plotted in figure 12 (for both 20 and 30 kc). They display a scatter of the same magnitude as the estimated error. The slope of the least-squares line through the points is only $0.003\,\mu A^{-1}$, a negligible quantity in the light of the scatter. A noteworthy point is that the values of t for zero illumination are distributed in much the same way as are those under illumination. If the diode is in thermal equilibrium, however, t must be unity, so the experimental points should scatter about t=1; i.e., some should lie above this value and some below. On the contrary, though, the experimental points representing results at zero illumination all lie above t=1, with an average value of 1.125.

The measurements indicated for $I_{sc}=0$ were made with the diode under negligible illumination. The galvanometer used to measure I_{sc} has a maximum sensitivity of $0.03\,\mu A/mm$ at a resistance of 360 ohms. With the diode in its 'dark' condition there was no measurable current reading on this meter. Since the diode's dark open-circuit resistance is much greater than 360 ohms, we may conclude that the 'dark' short-circuit current is less than $0.01\,\mu A$, which is about 1/30 of I_o. This indicates that the diode was in thermal equilibrium and hence should have had a noise temperature ratio of unity.

The small discrepancy noted in the zero illumination points of figure 12, therefore, must be ascribed to some systematic error in the measurement procedure arising probably from calibration discrepancies between the reference resistance box and the impedance

bridge at the frequencies used. If this systematic error is now subtracted from the values of t under illumination it is seen that even at the maximum illumination level t would not exceed 1.12.

The important feature of the noise measurements is that the open-circuit noise temperature ratio is very nearly unity and varies negligibly over a short-circuit current range from zero to over 130 times I_o. This result is in very good agreement with that predicted in section 1.2, and suggests that the simple assumptions made therein are quite adequate to predict the noise behavior of open-circuited ideal photo-diodes when subjected to intense illumination which produces a very large departure from the equilibrium values of the carrier densities and flows and of the potential distribution.

It might be thought that we have considered only the noise arising in the diode itself and have neglected that inherent in the incident illumination. This is not the case, however, since in our theoretical discussion of shot noise in an illuminated diode we wrote (page 8):

$$\frac{\overline{i^2}}{\Delta f} = 2q(I_o \exp\frac{qV}{kT} + I_o + BL);$$

The first two current terms determine the diode's noise in thermal equilibrium, while the last (BL) accounts for the extra current flow due to illumination. Thus the photo-pair-production takes place at a mean rate $\frac{BL}{q}$ and the resulting current adds its shot noise contribution to that existing in equilibrium. In other words, a photo-hole-electron pair is created only when a photon is incident; thus the photocurrent includes the randomness of the incident illumination.

FIGURE 13

PHOTO-DIODE EQUIVALENT CIRCUITS

FOR SIGNAL AND NOISE IN OPEN-CIRCUIT OPERATION

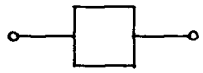

D.C. Generator (voltage or current)

Noise Generator (voltage or current)

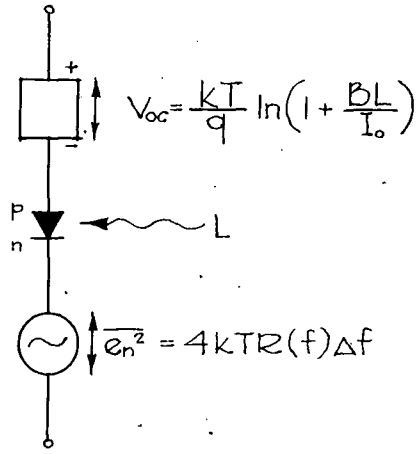

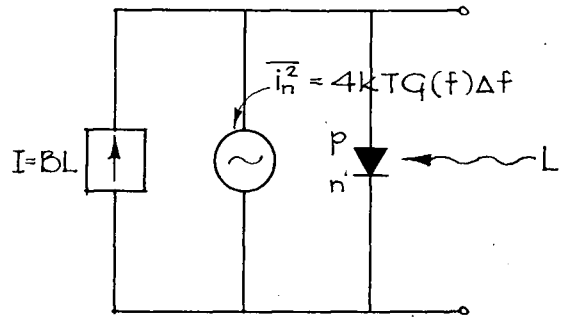

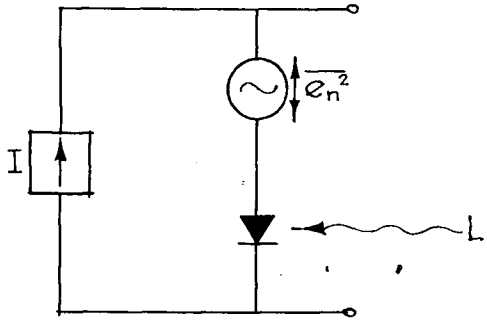

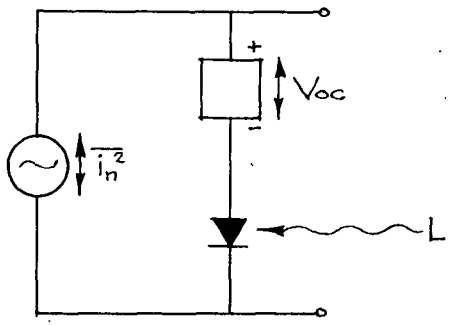

CHAPTER 4 - CONCLUSIONS

4.1 General Comments

The results of this investigation strongly suggest that the noise of an open-circuited ideal photo-diode may be regarded as thermal noise arising from random carrier motion across the junction. The additional carriers produced by the illumination change both the junction impedance and the mean-squared noise current in such a fashion that, providing the mean current is zero (i.e. open-circuit conditions), the noise remains equal to that ascribed by Nyquist's theorem to thermal fluctuations in the junction impedance. This is consistent with the rapid thermalization of the additional carriers by the very numerous collisions with the crystal lattice during their lifetime.

In view of these results, the simple representations shown in figure 13 describe the photovoltaic and noise generation of an ideal, open-circuited diode.

The fact that no excess noise (above thermal) was noted suggests that the ideal photo-diode should be an excellent radiation detector. The signal voltage obtained from one of these devices is 'free'; that is, no current need be supplied the device from an external source, as is necessary to develop a signal across a photoconductive detector. Excess current noise, therefore, does not appear at the photo-diode terminals. It should be emphasized, however, that this freedom from excess noise applies only under open-circuit conditions and, as is indicated by equation 4 (page 8), additional current noise will be observed if the diode is used to deliver current to a load.

Another point worth emphasizing is the condition applied

throughout that the diode be ideal. When a diode is being chosen for use as an open-circuit photovoltaic detector, it might seem reasonable to use for responsivity considerations its open-circuit voltage versus illumination characteristics and to neglect the form of its general current-voltage characteristic. This investigation, however, indicates that in addition the diode must be ideal (i. e. be characterized by equation 2, page 1) throughout the open-circuit voltage range in question. It may then be expected to display a higher signal-to-noise ratio under a given illumination than a non-ideal diode of higher absolute responsivity. The latter may have internal shunt paths causing a net flow of current through the junction due to circulating flow even though no external current flows. The treatment given earlier (equation 4) then indicates that the effective noise temperature ratio will exceed unity, implying a poorer sensitivity.

4.2 Design Recommendations for Radiation Detectors

Using the results of earlier analyses, we can draw several conclusions of value in designing a photo-diode for open-circuit detection application.

The open-circuit signal voltage appearing across the diode under illumination is

$$V_S = \frac{kT}{q} \ln\left(1 + \frac{BL}{I_o}\right)$$

and the r.m.s. noise voltage appearing with it in a bandwidth Δf is:

$$V_N = \left(4kT\Delta f R(\omega)\right)^{1/2}.$$

In the majority of detection applications the frequency range of interest will extend no higher than several kilocycles per second so we need only consider noise in this low frequency band ($\omega\tau \ll 1$). In this case and under open-circuit conditions

$$R(\omega) = \frac{\partial V}{\partial I} = \frac{kT}{qI_o} \exp\left(-\frac{qV_{oc}}{kT}\right)$$

$$= \frac{kT}{qI_o}\left(1 + \frac{BL}{I_o}\right)^{-1}$$

and hence $$V_N = 2kT\sqrt{\frac{\Delta f}{qI_o}}\left(1 + \frac{BL}{I_o}\right)^{-1/2}$$

Thus we may write the open-circuit signal-to-noise (voltage) ratio as

$$\frac{V_S}{V_N} = \left[\frac{I_o + BL}{4q\Delta f}\right]^{1/2} \ln\left(1 + \frac{BL}{I_o}\right).$$

At the limit of sensitivity, $BL \ll I_o$, so the signal-to-noise ratio becomes

$$\frac{V_S}{V_N} = \frac{BL}{2(qI_o\Delta f)^{1/2}} \quad . \tag{9}$$

To consider the implications of this equation on detector design we will assume that the diode is illuminated evenly over the entire junction area A so that B can be written in the form bA.

Assuming a p^+-n structure, we have (page 7):

$$I_o = Aqp_n\frac{D_P}{L_P} = Aqp_n\sqrt{\frac{D_P}{\tau_P}}$$

so that

$$\frac{V_S}{V_N} = \frac{bL}{2q}\left[\frac{A}{p_n\Delta f}\sqrt{\frac{\tau_P}{D_P}}\right]^{1/2} \qquad (10)$$

Evidently then, to secure the most favourable signal-to-noise ratio the following conditions should be met:

1. A should be large (for unfocussed radiation)
2. p_n should be small
3. τ_P should be large
4. D_P should be small.

The area A of the junction is limited by the optical system used to provide the signal illumination, the space available for the detector, and the technique used in producing the junction. These factors lie beyond the scope of this investigation. It should be noted, though, that if a certain total amount of incident radiation is available - that is, if BL is fixed - the maximum signal-to-noise ratio will be attained by focussing this radiation on as small an area as possible so as to make $bLA^{1/2}$ large for a given value of bLA.

The minority carrier density p_n is related to the energy gap of the semiconductor E_g by the relation

$$p_n = \frac{K}{n_n}\exp\left(-\frac{E_g}{kT}\right)$$

where K is a constant for the purposes of this discussion. Hence p_n can be reduced by choosing a material with a large energy gap. It must be remembered, however, that the diode is photovoltaic only for photons of energy greater than the energy gap, so that E_g must be less than or equal to $h\nu$ for the radiation to be detected. Hence for a monochromatic

radiation detector it is advantageous to choose $E_g = h\nu$.

Reduction of p_n is also effected by heavy doping of the n region. This will generally cause only a negligible decrease in τ_p, the minority carrier lifetime and in D_p, the diffusion constant for holes in this region. A decrease in temperature will produce fewer thermal pairs in the n region and thus a cooled detector will display a more favourable signal-to-noise ratio.

Since the diffusion constant and the mobility of holes in the n region are related by the Einstein equation

$$D_p = \frac{kT}{q}\mu_p,$$

D_p may be reduced by choosing a material in which μ_p is small.

A typical maximum sensitivity may be calculated by use of suitable values in equation 9. For example, the following values lead to a value for the reverse saturation current I_o equal to $0.3\,\mu A$:

$A = 0.005\ cm^2$

$p_n = 3 \times 10^{11}\ cm^{-3}$ (corresponding to 1 ohm-cm n-type Ge at 300 K.)

$D_p = 45\ cm^2 sec^{-1}$ (Ge at 300 K)

$\tau_p = 30 \times 10^{-6}$ sec (value found experimentally)

The minimum detectable power, defined as the incident photon energy in a unit bandwidth which will give unity signal-to-noise ratio, is

$$P = \frac{E_g}{q}(BL)_{\frac{V_s}{V_N}=1} = 2E_g\left(\frac{I_o}{q}\right)^{1/2}$$

when the incident radiation is monochromatic and of frequency $\frac{E_g}{h}$. For germanium, $E_g = 0.7$ eV corresponding to a radiation wavelength of $1.8\,\mu$. Thus a germanium diode with the above-mentioned reverse saturation current of $0.3\,\mu A$ has a minimum detectable power P equal to 3×10^{-13} watt.

An excellent photoconductive cell noted in the literature (Smith, Jones, and Chasmar, 1957) has a minimum detectable power, when cooled, of 6.4×10^{-14} watt. It appears, then, that the ideal open-circuited p-n photo-diode can compete favourably with photoconductive devices in sensitivity and has the added advantage of requiring no external power supply.

APPENDIX

Shift in DC Bias Due to Rectification of AC Signal from Measuring Bridge

Consider the circuit shown below:

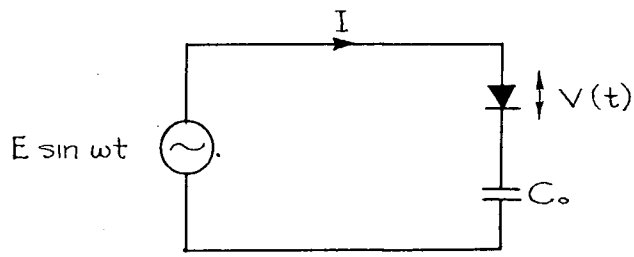

Now we know $$I = I_o(\exp\frac{qV}{kT} - 1) - BL \qquad (2)$$

and we will assume that the voltage across the diode V consists of two parts; i. e. $V = V_o + V_1 \sin\omega t$.

Hence $$I = I_o\left[\exp\frac{q}{kT}(V_o + V_1 \sin\omega t) - 1\right] - BL \ .$$

If we assume the ac part of the voltage across the diode is small so that $V_1 \ll \frac{kT}{q}$, this expression may be expanded to give

$$I = I_o(\exp\frac{qV_o}{kT} - 1) - BL$$

$$+ I_o\exp\frac{qV_o}{kT}\left[\frac{qV_1}{kT}\sin\omega t + \left(\frac{qV_1}{2kT}\right)^2(1 - \cos 2\omega t)\right]$$

and hence the average current $\langle I\rangle$ is given by

$$\langle I\rangle = I_o(\exp\frac{qV_o}{kT} - 1) - BL + (I_o\exp\frac{qV_o}{kT})\left(\frac{qV_1}{2kT}\right)^2 .$$

Because of the condenser in the circuit, however, the average current must be zero. Therefore:

$$\exp\frac{qV_o}{kT}\left[1 + \left(\frac{qV_1}{2kT}\right)^2\right] = 1 + \frac{BL}{I_o} .$$

The dc portion V_o of the voltage across the diode is made up of the photovoltage due to illumination and the bias shift (ΔV) due to rectification of the ac signal from the bridge. That is:

$$V_o = \frac{kT}{q}\ln(1 + \frac{BL}{I_o}) + \Delta V .$$

Hence $$\exp\frac{qV_o}{kT} = (1 + \frac{BL}{I_o})\exp\frac{q\Delta V}{kT} ,$$

and if the bias shift due to rectification is small ($\Delta V \ll \frac{kT}{q}$), then

$$\exp\frac{qV_o}{kT} \simeq (1 + \frac{BL}{I_o})(1 + \frac{q\Delta V}{kT}) .$$

By substitution of this result into equation 11 above it may readily be shown that:

$$\Delta V = -\frac{qV_i^2}{4kT} .$$

The conductance G_m actually measured by the bridge is given by

$$G_m = \left.\frac{\partial I}{\partial V}\right|_{oc} = \frac{qI_o}{kT}\exp\frac{qV_o}{kT}$$

$$= \frac{qI_o}{kT}(1 + \frac{BL}{I_o})\exp\frac{q\Delta V}{kT}$$

$$= G_o(0)\exp\frac{q\Delta V}{kT}$$

$$\simeq G_o(0)(1 + \frac{q\Delta V}{kT})$$

$$= G_o(0)\left[1 - \left(\frac{qV_i}{2kT}\right)^2\right].$$

Hence if $V_i = 25$ mv, $G_m = 0.75G_o(0)$

$V_i = 10$ mv, $G_m = 0.96G_o(0)$

$V_i = 5$ mv, $G_m = 0.99G_o(0)$.

In this last case, $V_i \ll \frac{kT}{q}$ and $\Delta V = 0.25$ mv which is also $\ll \frac{kT}{q}$ so the assumptions made in the derivation are valid.

BIBLIOGRAPHY

Cummerow, R. L., "Photovoltaic Effect in p-n Junctions", Physical Review, 95, p. 16 (July 1, 1954).

Gianola, U. F., "Photovoltaic Noise in Silicon Broad Area p-n Junctions", Journal of Applied Physics, 27, p. 51 (January, 1956).

Misawa, T., "Emitter Efficiency of Junction Transistor", Journal of the Physical Society of Japan, 10, p. 362 (May, 1955).

Mitchell, G. R., Goldberg, A. E., and Kurnich, S. W., "InSb Photovoltaic Cell", Physical Review, 97, p. 239 (January, 1955).

Pearson, G. L., Montgomery, H. C., and Feldmann, W. L., "Noise in Silicon p-n Junction Photocells", Journal of Applied Physics, 27, p. 91 (January, 1956).

Shockley, W., "The Theory of p-n Junctions in Semiconductors and p-n Junction Transistors", Bell System Technical Journal, 28, p. 435 (July, 1949).

Smith, R. A., Jones, F. E., and Chasmar, R. P., "The Detection and Measurement of Infra-red Radiation", Oxford University Press, 1957.

Tauc, J., "Generation of an emf in Semiconductors with Nonequilibrium Current Carrier Concentrations", Reviews of Modern Physics, 29, p. 308 (July, 1957).

Torrey, H. C., and Whitmer, C. A., "Crystal Rectifiers", McGraw-Hill Book Company, Inc., 1948.